Sieber, J. (2006). Dynamics of delayed relay systems. 10.1088/0951-7715/19/11/001

Dynamics of delayed relay systems

J Sieber

Bristol Centre of Applied Nonlinear Mathematics, Dept. of Engineering Mathematics, University of Bristol, U.K.,

E-mail: jan.sieber@bristol.ac.uk

Abstract. The paper studies the dynamics near periodic orbits in dynamical systems with relays (switches) that switch only after a fixed delay. As a motivating application, we study the problem of stabilizing an unstable equilibrium by feedback control in the presence of a delay in the control loop. We show that saddle-type equilibria can be stabilized to a periodic orbit by a switch even if this switch is subject to an arbitrarily large delay. This is in contrast to linear static feedback control, which fails when the delay is larger than a problem-dependent critical value. Our analysis is based on the reduction of the return map near a generic periodic orbit to a finite-dimensional map. This map is smooth if the periodic orbit satisfies two genericity conditions. A violation of any of these two conditions causes a discontinuity-induced bifurcation of the periodic orbit. We derive asymptotic expressions for the piecewise smooth return map for each of these two codimension-one bifurcations. This analysis shows that the introduction of a small delay into the switching decision can induce chaos in a relay system that had a single stable periodic orbit without delay. This small-delay behaviour is fundamentally different from smooth dynamical systems.

AMS classification scheme numbers: 37G15, 34K18, 34K35

1. Introduction

This paper is concerned with dynamical systems with delayed relays. Relay systems follow two different smooth vector fields in two different regions of their physical space. Specifically, we consider the effects of a time delay in the decision when to switch from one vector field to the other. As an initial motivation let us consider the problem of stabilizing an unstable equilibrium by feedback in the presence of delay in the feedback loop, which is a typical situation in applications. For example, a controlled inverted (massless and frictionless) pendulum on a cart, as shown in figure 1, is governed by the equation

$$\ddot{\theta} = \sin\theta - F\cos\theta. \tag{1}$$

In (1), the dependent variable θ is the inclination angle of the pendulum. The force F is applied as a feedback to the cart with the goal of stabilizing the unstable upright position $\theta = 0$; see figure 1. Time has been rescaled to units of $\sqrt{2L/(3g)}$ in (1) where L is the length of the pendulum and g describes the gravitational acceleration. This implies that a fixed reaction time in the application of the feedback force $F(\theta, \dot{\theta})$ gives a delay τ in the arguments of F which increases for decreasing L. The inverted pendulum is a prototype for balancing tasks in robotics and biomechanics [1, 2], and

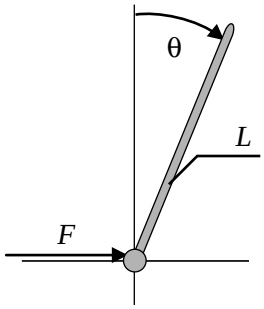

Figure 1. Sketch of the setup for the controlled inverted pendulum on a cart.

a textbook example in control theory [3] and the study of delay effects [4]. Let us consider the following question:

Problem 1 (Balancing) *Let $\tau > 0$ be a given, potentially large, delay. Find a function $F : \mathbb{R}^2 \to \mathbb{R}$ such that the feedback law $F(\theta(t-\tau), \dot{\theta}(t-\tau))$ inserted into (1) is able to stabilize the upright position $\theta = 0$.*

For linear F this is impossible as soon as the delay τ exceeds a certain critical value τ_c. The critical delay $\tau_c = \sqrt{2}$ is derived in the textbook [4] for the classical PD control law $F(\theta(t-\tau), \dot{\theta}(t-\tau)) = a\theta(t-\tau) + b\dot{\theta}(t-\tau)$. The works [5, 6] have found critical delays also for other specific linear control laws. Reference [7] presents a complete stabilizability analysis for two-dimensional linear systems with static feedback subject to time-delay, giving the critical delay in dependence of all relevant system parameters. The references [8, 9] include small oscillations and other nonlinear phenomena, which occur for delays close the critical value, into their study. A conclusion of [6] is that, even if one accepts small stable oscillations around the upright position as successful balancing, the restriction on the delay cannot be relaxed substantially beyond the critical value obtained from the linear theory.

In order to overcome this fundamental restriction, we consider a relay switch in (1) of the form

$$F = \varepsilon \mathrm{sgn}[g(\theta(t-\tau), \dot{\theta}(t-\tau))], \tag{2}$$

where $g : \mathbb{R}^2 \to \mathbb{R}$ is a smooth or piecewise affine function dividing $\mathbb{R}^2$ into two simple domains $G_1 = \{g < 0\}$ and $G_2 = \{g \geq 0\}$. A feedback of the form (2) can never stabilize the equilibrium $\theta = 0$ perfectly but will, at best, admit small stable oscillations that switch back and forth between $F = \varepsilon$ and $F = -\varepsilon$ [10]. If we accept small oscillations as successful balancing then a relay switch F of the form (2) can achieve stabilization [11]. Surprisingly, one can even construct a stabilizing feedback of form (2) for any given delay τ, thus, removing any restriction on the delay. In section 5 we will give a geometric illustration how to construct the switching function g for a given delay τ for the inverted pendulum (1) and prove the following general result:

Theorem 2 (Existence of stable periodic orbits) *Let $f : \mathbb{R}^n \times \mathbb{R} \to \mathbb{R}^n$ be smooth and let $\dot{x} = f(x, 0)$ have a saddle equilibrium x_0. Let $\tau > 0$ be arbitrarily large and $\varepsilon > 0$ be sufficiently small. If the pair $(\partial_x f(x_0, 0), \partial_u f(x_0, 0))$ is controllable then there exists a smooth function $g : \mathbb{R}^n \to \mathbb{R}$ such that*

$$\dot{x} = f(x, \varepsilon \mathrm{sgn}[g(x(t-\tau))])$$

has a stable periodic orbit.

The only condition on $(\partial_x f(x_0,0), \partial_u f(x_0,0))$, apart from the saddle type of x_0, is controllability (which is a genericity condition), which is obviously necessary. The key point of Theorem 2 is that controllability is also sufficient. The stable periodic orbit is in a neighbourhood of x_0 of order ε. In the formulation of Theorem 2 the switching law g depends on ε and τ. In particular, a function g that guarantees a stable periodic orbit for a certain large delay τ does not necessarily also guarantee a stable periodic orbit for all smaller τ.

A crucial ingredient in the proof of Theorem 2 is a precise description of the dynamics near periodic orbits of a general n-dimensional system of differential equations of the form

$$\dot{x}(t) = \begin{cases} f_1(x(t)) & \text{if } g(x(t-\tau)) < 0 \\ f_2(x(t)) & \text{if } g(x(t-\tau)) \geq 0 \end{cases} \tag{3}$$

where $\tau > 0$ is the delay in the switching decision. The presence of the delay in (3) gives rise to an infinite-dimensional phase space, the space $C([-\tau, 0]; \mathbb{R}^n)$ of continuous functions on the history interval $[-\tau, 0]$. However, if a periodic orbit $\tilde{x}(\cdot)$ of (3) switches only finitely often per period and satisfies two genericity conditions then the dynamics of (3) near $\tilde{x}(\cdot)$ is described by a smooth finite-dimensional local return map. In short, the genericity conditions are that

(i) all intersections of the periodic orbit $\tilde{x}(\cdot)$ with the switching manifold $\{g = 0\}$ are transversal, and

(ii) along the periodic orbit $\tilde{x}(\cdot)$ none of the delayed switching events coincides with a crossing of the switching manifold $\{g = 0\}$ (that is, if $g(\tilde{x}(s)) = 0$ then $g(\tilde{x}(s+\tau)) \neq 0$ for all $s \in \mathbb{R}$).

We will derive a precise relation between the dimension of the image of the return map and the location of the switching times of the orbit $\tilde{x}(\cdot)$. In particular, this dimension is $n-1$ (where n is the dimension of the physical space of (3)) if all switching times along $\tilde{x}(\cdot)$ are separated by more than the delay time τ. This kind of the periodic orbits is called *slowly oscillating*. The finite-dimensionality of the local return maps of periodic orbits is in contrast to the situation in smooth delay differential equations (DDEs) where periodic orbits typically have infinitely many non-zero Floquet multipliers [12].

The second main result of the paper gives a complete description of possible discontinuity-induced bifurcations of codimension one for a slowly oscillating periodic orbit $\tilde{x}(\cdot)$. Each of these bifurcations corresponds to a violation of one of the genericity conditions (i) and (ii). Violation of condition (i) implies generically that $\tilde{x}$ grazes (touches) the switching manifold $\{g = 0\}$ quadratically. This induces a return map for $\tilde{x}$ that is asymptotically linear on one side of the grazing manifold and square-root like on the other side. This square-root asymptotics implies that the introduction of a small delay into the switching decision of a relay system can change the dynamics drastically. In particular, it can introduce chaos into a system that, without delay, has a stable periodic orbit as its only attractor. This small-delay limit behaviour is fundamentally different from the case of smooth DDEs and will be illustrated with a more detailed example in section 6.3. The violation of condition (ii) corresponds to a corner collision and gives rise to a piecewise asymptotically linear return map near the colliding periodic orbit $\tilde{x}$. This reduction to piecewise smooth finite-dimensional maps links the local bifurcation theory of periodic orbits in delayed relay systems

to the well-established results of the bifurcation theory for piecewise smooth maps [13, 14, 15, 16].

The paper is organized as follows. Section 2 outlines how the results of this paper relate to previous and recent studies on the dynamics of piecewise smooth ordinary and delay differential equations, and how the result of Theorem 2 relates to common delay compensation techniques in control theory and engineering. Section 3 revisits some common notation for the definition of the forward evolution of DDEs, also pointing out the differences to the case of smooth DDEs. Section 4 shows under which conditions the local return map of a periodic orbit reduces to a finite dimensional smooth map. Section 5 first shows how one can construct a switching law g in (2) that gives rise to a stable periodic orbit for the inverted pendulum in the presence of an arbitrary delay. This construction reveals already the main ideas of the proof for the general result in Theorem 2. The section also lists the main differences between the illustrating example and the general n-dimensional case. The detailed proof of Theorem 2 can be found in Appendix C. Section 6 studies the two codimension-one bifurcations of slowly oscillating periodic orbits, stating secondary non-degeneracy conditions and deriving asymptotic expressions for the return maps. The sections 4, 5 and 6, which contain technical material and general theoretical results, include also simple but instructive examples illustrating the main concepts and ideas. More technical parts of the proofs for statements in the sections 4, 5 and 6 are given in separate appendices.

2. Background

Piecewise smooth dynamical systems model many problems in control engineering [17, 18], in mechanics (for example in systems with dry friction [19] or impacts [20]), in electrical systems with switches [21], or in biological systems with threshold effects [22]. In these situations one observes an evolution that is governed by different smooth vector fields in different regions of the phase space, which are separated by switching manifolds. These hybrid systems are an attractive subject of study as they can generate complex dynamics even if all of the vector fields and switching manifolds are simple enough (for example linear) to study them analytically. Moreover, they show phenomena such as chaotic attractors robustly, which are often non-hyperbolic and, thus, extremely subtle, in smooth maps and vector fields. This feature allows one to 'engineer' particular dynamics such as chaos [16]. In control theory piecewise linear systems are used to approximate nonlinear systems to understand the global dynamics and guarantee global stability [17]. See [14] for a survey on the active development of general bifurcation theory for piecewise smooth dynamical systems.

Whenever the non-smoothness of the dynamical system is induced by the implementation of a switch one can expect that the actual switch is subject to a delay, giving rise to delayed relay models such as (3). In applications this delay is often artificially increased (or hysteresis is introduced) since otherwise so-called 'sliding' along the switching manifold can occur, which would involve are large number of switchings in a short time interval [18].

The works [10, 23] studied one-dimensional prototype examples of the form

$$\dot{x} = \kappa\, x - \mathrm{sgn} x(t-\tau), \quad (\kappa > 0), \tag{4}$$

and found that this type of system typically admits periodic orbits that switch back and forth between the two vector fields. Moreover, they have classified all possible dynamics of system (4) completely and also studied its behaviour with respect to

perturbations, including periodic forcing. The references [24, 25, 26] have studied other simple piecewise linear systems (typically with a two-dimensional physical space). In contrast to the studies of (4) these investigations have found a huge variety of different dynamics such as chaos [26] or a complex network of periodic orbits [24, 25]. The different regimes are connected by grazing or collision events that show similarities to those in impacting or dry-friction systems [14]. However, even the behaviour of simple prototype systems such as studied in [24, 25, 26] is far from being classified completely.

In this paper we adopt a different approach. We consider a general system of form (3) and assume that it has a periodic orbit $\tilde{x}(t)$ ($t \in [-p, 0]$) that has a finite number of switchings between the vector fields. Then we study the dynamics near this periodic orbit and its bifurcations. In this way the results of our paper will be more general than studies of specific classes of examples such as [10, 24, 25, 26] but all statements are valid only locally. The consideration of only two vector fields in (3) is not really a restriction when one studies the local dynamics near a particular periodic orbit.

A further motivation for the study of the general system (3) is its connection with smooth delay differential equations (DDEs) with steep nonlinearities. Often one can start from (3) as a limiting case where the existence of stable periodic orbits is easy to prove and then deduce the persistence of these orbits for smooth DDEs close to (3) [27]. Reference [24] also continued periodic orbits of (3) approximately by standard numerical software for smooth DDEs after 'smoothing' the discontinuity in (3). The limit turns out to be well-behaved if the periodic orbit is not close to one of the bifurcations discussed in section 6.

Finally, let us put Problem 1 and Theorem 2 into perspective compared to classical delay compensation techniques in control theory and engineering. The studies [4, 5, 6, 7] and Theorem 2 are restricted to static feedback. That is, the feedback law (for example F in (1)) is only a function of a single instance of the delayed state. Classical delay compensation techniques that can cope with an arbitrarily large delay rely on dynamic feedback where the feedback depends on a predictor, obtained by a real-time solution of a functional equation (see, for example, [28, 29]). The fact that the basin of attraction of the periodic orbit in Theorem 2 will, in general, be exponentially small for large delay τ is only formally a difference to classical dynamic feedback schemes. Even though methods based on functional predictors can be globally asymptotically stable on the linear level, they have exponentially large transients if the initial condition is not already exponentially close to the equilibrium. See also [30] for a survey on implementation problems of functional predictors and how to overcome them. In the case of small delays polynomial forward prediction, such as used in substructuring [31, 32] in civil and mechanical engineering, is often successful and easier to implement in real-time.

3. Fundamental properties of delayed relay systems — definition of forward evolution

We define a delayed relay system as a dynamical system governed by a differential equation of the form (3) where $\tau > 0$, and $f_1, f_2 : \mathbb{R}^n \to \mathbb{R}^n$ are Lipschitz continuous. We assume that the switching function $g : \mathbb{R}^n \to \mathbb{R}$ is a piecewise smooth Lipschitz continuous function. Furthermore, we assume that the gradient $g'(x)$ is non-zero whenever it exists and $g(x)$ is zero. These assumptions on g imply that the set

$\{x : g(x) = 0\}$ constitutes a piecewise smooth $(n-1)$-dimensional submanifold of $\mathbb{R}^n$, which we call the *switching manifold*.

We denote the n-dimensional flow corresponding to f_j $(j = 1, 2)$ by Φ_j. That is, the time-t map generated by $\dot{x} = f_j(x)$ is $\Phi_j(t;\cdot) : \mathbb{R}^n \to \mathbb{R}^n$.

When solving differential equations where the right-hand-side depends also on the state in the past one typically has to keep track of the solution history along the trajectory [12]. Thus, the natural phase space, also for a system of the form (3), is the space $C([-\tau, 0]; \mathbb{R}^n)$ of continuous functions on the closed interval $[-\tau, 0]$. This section is concerned with the definition of the forward evolution $E(t;\cdot)$ for (3), which maps an initial value $x_0 \in C([-\tau, 0]; \mathbb{R}^n)$ to its time-T image $E(T; x_0) \in C([-\tau, 0]; \mathbb{R}^n)$.

In the case of a single delayed argument with a fixed delay τ as in (3) an intuitive way to define $E(T; x_0)$ is the method of steps [12, 33]: treat the past $x_0(t)$ $(t \in [-\tau, 0])$ as an inhomogeneity, solve the ensuing ordinary differential equation (ODE) for all times up to τ, and then shift the history and repeat the process.

For example, consider an initial history segment $x_0 \in C([-\tau, 0]; \mathbb{R}^n)$ that intersects the switching manifold only finitely many times, that is, $g(x_0(t-\tau)) = 0$ only for $t = t_1, \ldots, t_\mu \in [0, \tau]$. This divides the interval $[0, \tau]$ into $\mu + 1$ subintervals I_k:

$$I_0 = (0, t_1], \quad I_k = (t_k, t_{k+1}] \text{ for } k = 1, \ldots, \mu - 1, \quad I_\mu = (t_\mu, \tau].$$

The forward evolution will follow one of the flows Φ_{j_k} ($j_k = 1$ or 2 for $k = 0, \ldots, \mu$) in each subinterval I_k. Thus, we can define the curve $x(t)$ for $t \in [0, \tau]$ recursively by

$$\begin{aligned} x(t) &= \Phi_{j_0}(t; x_0(0)) \quad \text{for } t \in I_0 \\ x(t) &= \Phi_{j_k}(t - t_k; x(t_k)) \quad \text{for } t \in I_k,\ k = 1 \ldots, \mu - 1, \\ x(t) &= \Phi_{j_\mu}(t - t_\mu; x(t_\mu)) \quad \text{for } t \in I_\mu. \end{aligned} \tag{5}$$

For any t in the interior of any of the intervals I_k the point $x(t)$ satisfies the differential equation (3) with the history x_0. Thus, the forward evolution $E(T; x_0) \in C([-\tau, 0]; \mathbb{R}^n)$ for $T \in [0, \tau]$ is defined by

$$E(T; x_0)(t) = \begin{cases} x(t+T) & \text{if} \quad t \in (-T, 0] \\ x_0(t+T) & \text{if} \quad t \in [-\tau, -T]. \end{cases} \tag{6}$$

For times $T > \tau$ we define $E(T;\cdot)$ as a concatenation of time steps smaller than τ, for example $E(T;\cdot) := E(T/(k+1);\cdot) \circ \ldots \circ E(T/(k+1);\cdot)$ when $T \in [k\tau, (k+1)\tau)$. This definition is independent of the particular partition of the interval $(0, T)$.

Recursion (5) reveals that the evolution $E(\cdot, x_0)$ does not depend on the complete shape of $x_0 \in C([-\tau, 0]; \mathbb{R}^n)$ but only on the position of $x_0(0) \in \mathbb{R}^n$ (the *headpoint* of x_0) and the finitely many switching times $t_1 - \tau, \ldots, t_\mu - \tau$ in the interval $[-\tau, 0]$. This suggests that the dynamics of delayed relay systems such as (3) is governed by only finitely many coordinates despite the infinite-dimensionality of the underlying phase space. This is generically the case near periodic orbits with only finitely many intersections of the switching manifold, which are discussed in section 4. The construction also shows that delayed relays cannot induce 'sliding', which is common in non-delayed systems of the form (3) (that is, if $\tau = 0$ in (3)).

The above construction of $E(\cdot; x_0)$ assumes that x_0 intersects the switching manifold only finitely many times within $[-\tau, 0]$. For many elements of $C([-\tau, 0]; \mathbb{R}^n)$ this is not the case. For general $x_0 \in C([-\tau, 0]; \mathbb{R}^n)$ we define the curve $x(t)$ as the

solution $x \in C([0,T];\mathbb{R}^n)$ of the variation-of-constants formula corresponding to DDE (3)

$$x(t) = x_0(0) + \frac{1}{2}\int_0^t f_1(x(s))\,[1-\operatorname{sgn} g(x_0(s-\tau)))] + \\ + f_2(x(s))\,[1+\operatorname{sgn} g(x_0(s-\tau))]\;ds. \tag{7}$$

In the integral equation (7) we use the convention that $\operatorname{sgn} 0 = 1$. Equation (7) has a unique solution $x \in C([0,T];\mathbb{R}^n)$ satisfying $x(0) = x_0(0)$ due to the Lipschitz continuity of f_1 and f_2 and the measurability of $\operatorname{sgn} g(x_0(\cdot))$. In general, the points $x(t)$ satisfy the differential equation (3) for t in the open and dense subset of $(0,T)$

$$\{t \in (0,T) : g(x_0(t-\tau)) < 0\} \cup \operatorname{int}\{t \in (0,T) : g(x_0(t-\tau)) \geq 0\}$$

where the notation int refers to the interior of a set. We remark that this set may not necessarily have full Lebesgue measure on the interval $(0,T)$. For general x_0 we use the solution x of (7) instead of the simple recursion (5) in the definition (6) of $E(T;x_0)$.

We observe that the evolution $E(T;x_0)$ depends continuously on T but, in general, it does not depend continuously on x_0. In fact, arbitrarily close to any $x_0 \in C([-\tau,0];\mathbb{R}^n)$ that intersects $\{g=0\}$ at least once (say, in $s_1 \in (-\tau,0)$) we find a $x_\varepsilon \in C([-\tau,0];\mathbb{R}^n)$ which has $g(x_\varepsilon(s)) = 0$ for all $s \in (s_1-\varepsilon, s_1+\varepsilon)$. In general, we cannot expect that $E(T;x_\varepsilon)$ is continuous in its second argument in x_ε. Thus, E is not a semiflow in the classical sense of [34].

4. Behaviour near generic relay periodic orbits

Although equation (3) does not define a semiflow we can often understand the dynamics generated by (3) near periodic orbits by studying smooth finite-dimensional maps. This section will explain in detail how this reduction near periodic orbits works in the simplest (but generic) case.

4.1. Illustration — linearized inverted pendulum

Let us consider the example of the inverted pendulum from the introduction to illustrate how the infinite-dimensional semiflow simplifies to a low-dimensional map close to a periodic orbit. Inserting the relay feedback (2) into the differential equation governing the controlled inverted pendulum leads to a system of form (3). In the consideration of small periodic orbits close to the upright position the nonlinearities in (1) can be regarded as small perturbations. If $\varepsilon \ll 1$ and after rescaling $(\theta,\dot\theta) = (\varepsilon x_1, \varepsilon x_2)$ the nonlinear equation (1) with (2) is a perturbation of order $\mathrm{O}(\varepsilon^2)$ of

$$\begin{aligned} \dot x_1(t) &= x_2(t) \\ \dot x_2(t) &= x_1(t) - \operatorname{sgn} g(x_1(t-\tau), x_2(t-\tau)). \end{aligned} \tag{8}$$

Any structurally stable periodic orbit found in (8) will persist under small perturbations, and, thus, after rescaling, also exist in the nonlinear system (1) for sufficiently small ε. This reduction of a piecewise smooth system to the piecewise linear system (8) is an expression of the general fact that many key features of piecewise smooth dynamical systems can already be found in piecewise linear systems [14] where they simply persist under the perturbation caused by a small nonlinearity. The two

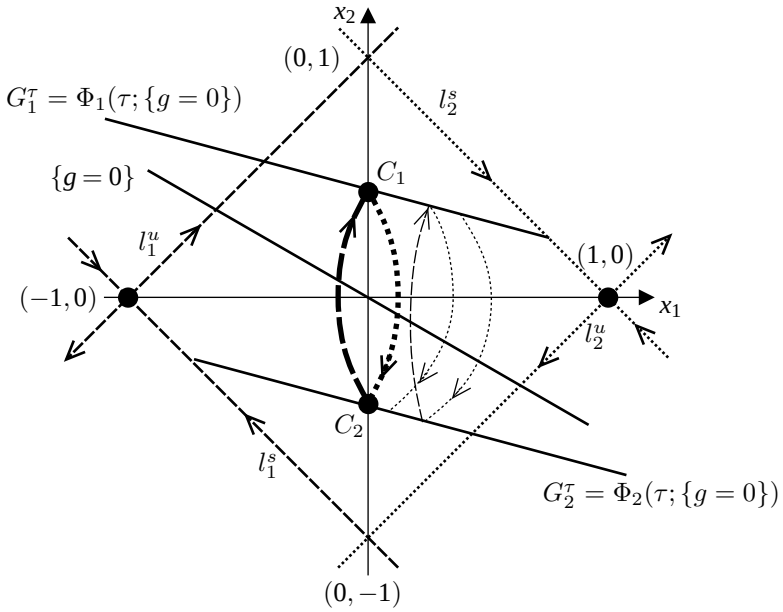

Figure 2. Sketch of the dynamics near a periodic orbit of the linearized inverted pendulum. The flows Φ_1 (dashed) and Φ_2 (dotted) are superimposed in $\mathbb{R}^2$. The periodic orbit is the bold closed curve with corners the C_1 and C_1. The return map to this orbit is a 1D map from G_1^τ back to itself.

flows Φ_1 and Φ_2 can be computed analytically for (8), giving rise to the affine maps

$$\Phi_1(t;v) = A(t)v - v_0(t), \text{ and } \quad \Phi_2(t;v) = A(t)v + v_0(t)$$

where

$$A(t) = \begin{bmatrix} \cosh(t) & \sinh(t) \\ \sinh(t) & \cosh(t) \end{bmatrix}, \quad v_0(t) = \begin{bmatrix} 1-\cosh(t) \\ -\sinh(t) \end{bmatrix}.$$

Let us choose, for illustration, a linear switching function g of slope α, namely

$$g(x_1,x_2) = x_1\cos\alpha + x_2\sin\alpha, \quad \alpha \in (0,\pi/2),$$

and consider a delay $\tau < \log(1+\tan\alpha)$. Figure 2 shows a sketch of the situation. The flows Φ_1 (dashed) and Φ_2 (dotted) are superimposed in the plane $\mathbb{R}^2$. The flow Φ_1 has a saddle equilibrium at $(-1,0)$, the flow Φ_2 has a saddle at $(1,0)$. The stable ($l^s_{1,2}$) and unstable ($l^u_{1,2}$) subspaces of both flows form a square, which is sketched in figure 2. We denote the $\Phi_1(\tau;\cdot)$-image of $\{g=0\}$ by G_1^τ and its intersection point with the axis $x_1=0$ by C_1. Correspondingly, the $\Phi_2(\tau;\cdot)$-image of $\{g=0\}$ is denoted by G_2^τ and its intersection point with the axis $x_1=0$ by C_2. The points C_1 and C_2 are mirror images of each other ($C_2=-C_1$). If $\tau < \log(1+\tan\alpha)$ they are also mapped onto each other by the flows. That is, $C_2 = \Phi_2(p/2;C_1)$, $C_1 = \Phi_1(p/2;C_2)$ where

$$p = 2\left[\tau + \log\left(\frac{\mathrm{e}^\tau\tan\alpha + 1 - \mathrm{e}^\tau}{\tan\alpha + 1 - \mathrm{e}^\tau}\right)\right]. \tag{9}$$

This implies that the closed curve $W = \Phi_1([0,p/2);C_2)\cup\Phi_2([0,p/2);C_1)$ is the graph of a periodic orbit of (8). Moreover, the dynamics near W are given by the return map to the line G_1^τ, which is a one-dimensional map. Any initial value $x \in C([-\tau,0];\mathbb{R}^2)$

that is sufficiently close to $\Phi_1([-\tau,0];C_1)$ will, after time τ, follow Φ_2. Thus, the next switching to Φ_1 will invariably be located on the time-τ image of $\{g=0\}$ under Φ_2, which is G_2^τ. From now on the trajectory will always follow Φ_1 to G_1^τ and Φ_2 to G_2^τ, reducing the evolution of (8) to a smooth one-dimensional map from G_1^τ back to itself. This map is nonlinear if $\alpha \neq \pi/4$ even though both flows and g are linear.

The facts that make this reduction possible are that

(i) the switchings of W (C_1 and C_2) have a positive distance from $\{g=0\}$,

(ii) the intersections of W with $\{g=0\}$ are transversal,

(iii) the time between successive crossings of the switching manifold is larger than the delay τ.

The first two conditions are genericity conditions. Their violations correspond to discontinuity induced bifurcations, which are discussed in section 6. Periodic orbits that satisfy the last condition are called slowly oscillating.

We observe that the same curve W is the graph of a periodic orbit also if the delay τ in (8) is replaced by a delay of size $\tau + kp$ where k is a positive integer and p is the period of W given in (9). Then all time differences between successive crossings of the switching manifold $\{g=0\}$ are smaller than the switching delay. Thus, W for delay $\tau+kp$ with $k \geq 1$ would be a *rapidly oscillating* periodic orbit. A general lemma expressing the return map will be developed in the following section. It also applies to rapidly oscillating orbits and gives for the pendulum case a dimension of $1+2k$ for the return map.

4.2. Return map for periodic orbits in the general case

Suppose that the evolution of (3) has a periodic orbit W of period p. We can assume that $p \geq \tau$ without loss of generality because we do not require p to be the minimal period. We denote the elements of W by $\tilde{x}_t$ where $\tilde{x}_t = E(t;\tilde{x}_0) \in C([-\tau,0];\mathbb{R}^n)$ for $t \in (0,p]$ and $\tilde{x}_p = \tilde{x}_0$, and denote the corresponding trajectory of headpoints $\tilde{x}_t(0)$ by $\tilde{x}(t)$. The closed curve $\tilde{x}([-p,0]) \subset \mathbb{R}^n$ comprises the graph of the periodic orbit in the physical space $\mathbb{R}^n$. The function $\tilde{x}(\cdot)$ can be extended to the whole real axis due to the periodicity of W. In the following paragraphs we formulate three fundamental assumptions on f_1, f_2, g and $\tilde{x}$. If f_1, f_2 and g are at least piecewise smooth functions then these conditions (3, 5, and 6) are genericity conditions on the periodic orbit.

Condition 3 (finitely many intersections with switching manifold)
We assume that the graph $\tilde{x}([-p,0]) \subset \mathbb{R}^n$ of the periodic orbit W intersects the switching manifold in at most finitely many points. That is, $g(\tilde{x}(\tilde{s}_k)) = 0$ for at most finitely many times $\tilde{s}_k$ ($k=1,\ldots,m$) in $(-p,0)$.

Then, $\tilde{x}([-p,0])$ is composed of $m+1$ curves following either Φ_1 or Φ_2 with switching (or touching) times $\tilde{t}_k = [(\tilde{s}_k+\tau) \bmod p] - p$. We can assume without loss of generality that the intersection times $\tilde{s}_k$ and the switching times $\tilde{t}_k$ lie in the open interval $(-p,0)$ for $k=1,\ldots,m$. The trajectory $t \to \tilde{x}(t)$ is differentiable for all $t \in [-p,0]$ except possibly in $\tilde{t}_k$ ($k=1,\ldots,m$).

The following lemma states that the evolution E is continuous with respect to initial conditions in all points of the periodic orbit W in the topology of the Banach space $C([-\tau,0];\mathbb{R}^n)$. As pointed out in section 3 this continuity statement is rather subtle. If $\tilde{x}(\cdot)$, the graph of W, has at least one intersection with the switching manifold, and if $f_1 \neq f_2$ in this intersection, we cannot find a whole open neighbourhood of W where $E(t;x)$ is continuous with respect to x.

Lemma 4 (Continuity of evolution in periodic orbits)
Let $t_0 \in \mathbb{R}$, $T > 0$ be arbitrary, and $\tilde{x}_{t_0}$ be an element of a periodic orbit with finitely many intersections of the switching manifold. Then, $E(T;x)$ is continuous with respect to $x \in C([-\tau,0];\mathbb{R}^n)$ in the point $x = \tilde{x}_{t_0}$. Moreover, this continuity is uniform in T for T in any finite interval $[0,T_0]$.

Lemma 4 exploits the fact all x close to $\tilde{x}_{t_0}$ in $C([-\tau,0];\mathbb{R}^n)$-topology follow the same flow as $\tilde{x}$ outside of small neighbourhoods of the finitely many time points $\tilde{t}_1,\dots,\tilde{t}_m,\tilde{t}_1+p,\dots,\tilde{t}_m+p,\dots$ Thus, the proof of continuity for all $T > 0$ relies strongly on the periodicity of $\tilde{x}(\cdot)$. The complete proof is included as Appendix A.

Due to the continuity stated in Lemma 4, it makes sense to define a local return map, or *Poincaré map*, for the periodic orbit W. It is defined as the map induced by the first return to a hyperplane in the phase space transversal to the periodic orbit. For simplicity of notation we restrict ourselves in all further considerations to return maps to hyperplanes defined by a condition on the headpoint $z(0)$ of a function $z \in C([-\tau,0];\mathbb{R}^n)$. Let $l_0 \in \mathbb{R}^n$ be a vector of length 1 such that $l_0^T\dot{\tilde{x}}(0) > 0$. The curve $\tilde{x}(\cdot)$ is differentiable in $t = 0$ because all switching times $\tilde{t}_k$ are different from 0. The Poincaré map is defined as the local return map from the hyperplane

$$\mathcal{H} := \{z \in C([-\tau,0];\mathbb{R}^n) : l_0^T[z(0) - \tilde{x}(0)] = 0\} \tag{10}$$

to itself. Locally, this is a well-defined map in the following sense.

There exist small open neighbourhoods $\mathcal{U}_0 \subset \mathcal{U}_1 \subset C([-\tau,0];\mathbb{R}^n)$ of $\tilde{x}_0$ ($\tilde{x}(0)$ is the headpoint of $\tilde{x}_0$) and a neighbourhood $(T_1,T_2) \subset \mathbb{R}$ of p such that

- $E(p;\mathcal{U}_0) \subset \mathcal{U}_1$, and
- for all $z \in \mathcal{H} \cap \mathcal{U}_0$, there exists a unique time $T(z)$ of first return to the set $\mathcal{U}_1 \cap \mathcal{H}$ within (T_1,T_2).

That is, $T(z)$ is defined as the minimal time in the interval (T_1,T_2) satisfying $l_0^T[E(T(z);z)(0) - \tilde{x}(0)] = 0$. This first return time $T(z)$ is a well defined function of z for all $z \in \mathcal{U}_0$. The return time $T(z)$ is continuous in the point $z = \tilde{x}_0$ but, in general, not in U_0 because not necessarily all trajectories starting in U_0 intersect $\mathcal{H}$ transversally. Hence, also the Poincaré map $P : \mathcal{U}_0 \cap \mathcal{H} \to \mathcal{U}_1 \cap \mathcal{H}$ defined by $Pz := E(T(z);z)$ is well defined in $\mathcal{H} \cap U_0$, is continuous in $z = \tilde{x}_0$, but not necessarily continuous in $\mathcal{H} \cap U_0$. Let us denote by $\mathcal{S}$ the domain of definition of P, the *local Poincaré section* $\mathcal{U}_0 \cap \mathcal{H}$.

Let $L \in \mathbb{R}^{n\times(n-1)}$ be such that the augmented matrix $[l_0 L] \in \mathbb{R}^{n\times n}$ is orthogonal. Thus, $l_0^T L v = 0$ for all $v \in \mathbb{R}^{n-1}$. The headpoints of elements of the local Poincaré section $\mathcal{S}$ all have the form $\tilde{x}(0) + Lv$ where $v \in \mathbb{R}^{n-1}$ is small.

The following two assumptions on the periodic orbit $\tilde{x}$ and the switching function g will allow us to reduce the Poincaré map P to a smooth finite-dimensional map.

Condition 5 (Smoothness in intersection points)
We assume that $g(\dot{\tilde{x}}(\tilde{t}_k)) \neq 0$ for all $k = 1,\dots,m$.

Condition 5 implies that the two sets of points $\{\tilde{x}(\tilde{s}_1),\dots,\tilde{x}(\tilde{s}_m)\}$ (where $\tilde{x}(\cdot)$ intersects the switching manifold) and $\{\tilde{x}(\tilde{t}_1),\dots\tilde{x}(\tilde{t}_m)\}$ (the corners of $\tilde{x}$, where $\tilde{x}(\cdot)$ actually switches) are disjoint. Furthermore, it implies that $\tilde{x}$ is differentiable in its intersections with the switching manifold at the times $\tilde{s}_k$ ($k = 1,\dots,m$). Thus, $\tilde{x}$ follows either Φ_1 or Φ_2 in $\tilde{s}_k$.

Condition 6 (Transversality of all intersections)
For all $k = 1, \ldots, m$ holds: The function g is differentiable in the vicinity of $\tilde{x}(\tilde{s}_k)$, and $g'(\tilde{x}(\tilde{s}_k))\dot{\tilde{x}}(\tilde{s}_k) \neq 0$. More precisely, if $\tilde{x}$ follows Φ_j in $\tilde{s}_k$ then $g'(\tilde{x}(\tilde{s}_k))f_j(\tilde{x}(\tilde{s}_k)) \neq 0$.

Condition 6 asserts that the switching manifold $\{g = 0\}$ is differentiable whenever it intersects the periodic orbit $\tilde{x}$. Moreover, Condition 6 asserts that the orbit $\tilde{x}$ intersects the switching manifold transversally in all its intersection points $\tilde{x}(\tilde{s}_k)$ $(k = 1, \ldots, m)$. Consequently, the number of switching times, m, must be even. We can assume that $\tilde{x}$ follows Φ_1 in $t = 0$ without loss of generality.

To fix notation, we number the intersection and switching times so that, for some $\mu \in \{0, \ldots, m\}$,

$$-\tau < \tilde{t}_1 < \ldots < \tilde{t}_\mu < 0, \text{ and } -p < \tilde{t}_{\mu+1} < \ldots < \tilde{t}_m < -\tau \tag{11}$$

with, correspondingly, $\tilde{s}_k = [(\tilde{t}_k - \tau) \bmod p] - p$. Thus, $\tilde{x}(\cdot)$ has the form

$$\tilde{x}(t) = \begin{cases} \Phi_1(t; \tilde{x}(0)) & \text{if } t \in [\tilde{t}_\mu, 0], \\ \Phi_2(t - \tilde{t}_k; \tilde{x}(\tilde{t}_k)) & \text{if } t \in [\tilde{t}_{k-1}, \tilde{t}_k) \text{ and } \mu - k \text{ is even}, \\ \Phi_1(t - \tilde{t}_k; \tilde{x}(\tilde{t}_k)) & \text{if } t \in [\tilde{t}_{k-1}, \tilde{t}_k) \text{ and } \mu - k \text{ is odd}, \\ \Phi_1(t + \tilde{t}_{\mu+1}; \tilde{x}(\tilde{t}_{\mu+1})) & \text{if } t \in [-p, \tilde{t}_{\mu+1}) \end{cases} \tag{12}$$

for $k \in \{1, \ldots, m\}$. Lemma 7 below states that the dynamics of the local Poincaré map $P : \mathcal{S} \to \mathcal{S}$ is attracted by a finite-dimensional local invariant manifold $\mathcal{M}$ after finite time. Moreover, the local manifold $\mathcal{M}$ can be parametrized by tuples $(v, t_1, \ldots, t_\mu) \in \mathbb{R}^{n-1+\mu}$ where each of the μ numbers t_k is close to $\tilde{t}_k$ and the vector $v \in \mathbb{R}^{n-1}$ is small. The number μ equals the number of switchings of the periodic orbit in the interval $[-\tau, 0]$ (see (11)). In the formulation of the lemma we use the notation that a set $\mathcal{M}$ is 'invariant under P relative to a set $\mathcal{N}$' if any trajectory starting in $\mathcal{M} \cap \mathcal{N}$ stays in $\mathcal{M} \cap \mathcal{N}$ under iterations of P as long as it stays in $\mathcal{N}$.

Lemma 7 *There exists an open neighbourhood $\mathcal{N}$ of $\tilde{x}_0$ in the local Poincaré section $\mathcal{S}$ that is mapped by $P^2 = P \circ P$ into a local manifold $\mathcal{M} \subset \mathcal{S}$ of dimension $n - 1 + \mu$ where μ is defined by (11). The local manifold $\mathcal{M}$ is invariant under P relative to $\mathcal{N}$. Moreover, $\mathcal{M}$ can be parametrized by a small open ball $\mathcal{B} \subset \mathbb{R}^{n-1+\mu}$ around $(0, \tilde{t}_1, \ldots \tilde{t}_\mu) \in \mathbb{R}^{n-1} \times \mathbb{R}^\mu$. The parametrization of $\mathcal{M}$*

$$\mathcal{I}_\mathcal{M} : (v, t_1, \ldots, t_\mu) \in \mathcal{B} \to z \in C([-\tau, 0]; \mathbb{R}^n) \tag{13}$$

is defined recursively by

$$z(t) = \begin{cases} \Phi_1(t; \tilde{x}(0) + Lv) & \text{if } t \in [t_\mu, 0], \\ \Phi_2(t - t_k; z(t_k)) & \text{if } t \in [t_{k-1}, t_k) \text{ and } \mu - k \text{ is even}, \\ \Phi_1(t - t_k; z(t_k)) & \text{if } t \in [t_{k-1}, t_k) \text{ and } \mu - k \text{ is odd} \end{cases} \tag{14}$$

where we use the notation $t_0 := -\tau$.

We note that the manifold $\mathcal{M}$ and even the number μ defining the dimension of $\mathcal{M}$ may depend on the choice of the hyperplane of the Poincaré section $\mathcal{H}$. The proof, which appears in full in Appendix B, is based on the fact that any initial condition sufficiently close to $\tilde{x}_0$ will also always intersect $\{g = 0\}$ transversally after one iteration of P. This gives rise to parametrization (14) in the second iteration of P. Description (14) of $\mathcal{M}$ expresses that, for elements z of $\mathcal{M}$, we have to store only the location v of the headpoint $(z(0) = \tilde{x}(0) + Lv)$ and the switching times within $(-\tau, 0)$, of which we have exactly μ if we are sufficiently close to the periodic orbit $\tilde{x}$.

Furthermore, $\mathcal{I}_\mathcal{M}$ induces a map P_0 on $\mathcal{B}$ defined by $\mathcal{I}_\mathcal{M} P_0 y = P\mathcal{I}_\mathcal{M}(y)$. If $\mathcal{B}$ is sufficiently small all intersections of the headpoint trajectory $E(t; \mathcal{I}_\mathcal{M}(y))(0)$ with the switching manifold are still transversal for all $y \in \mathcal{B}$. Thus, P_0 is differentiable and the smoothness of P_0 is only limited by the smoothness of the switching function g and the flows Φ_j. Hence, if f_j and g are differentiable to a higher degree then P_0 is as well.

We remark that the decay to zero in finite time for certain components of the infinite-dimensional initial condition is a common feature also in smooth delay differential equations. This phenomenon manifests itself in the existence of 'small solutions'; see [33] for a comprehensive discussion in a textbook.

4.3. Poincaré map P_0 for slowly oscillating orbits

For slowly oscillating periodic orbits the manifold $\mathcal{M}$ simplifies to the local manifold in $\mathbb{R}^n$

$$G_0 := \{z \in \mathbb{R}^n : l_0^T (z - \tilde{x}(0)) = 0\} \cap U(\tilde{x}(0)),$$

where we denote by $U(\xi)$ a sufficiently small neighbourhood of a point $\xi \in \mathbb{R}^n$. The intersection times $\tilde{s}_k$ are separated by more than the delay time τ. This means that, without loss of generality, we can order the switching times as

$$-p < \tilde{s}_1 < \tilde{t}_1 = \tilde{s}_1 + \tau < \tilde{s}_2 < \tilde{t}_2 = \tilde{s}_2 + \tau < \ldots < \tilde{s}_m < \tilde{t}_m = \tilde{s}_m + \tau < 0. \tag{15}$$

Introducing the *local switching manifolds* (that is, local neighbourhoods of $\tilde{x}(\tilde{s}_j)$ within the switching manifold $\{g = 0\}$) and their time-τ images (in the same way as for the pendulum in section 4.1 and figure 2)

$$\begin{aligned} G_j &:= \{g = 0\} \cap U(\tilde{x}(s_j)) \quad \text{for } j = 1, \ldots, m \\ G_j^\tau &:= \Phi_1(\tau; G_j) \quad \text{for } j = 1, 3, \ldots, m-1 \text{ (odd)}, \\ G_j^\tau &:= \Phi_2(\tau; G_j) \quad \text{for } j = 2, \ldots, m \text{ (even)}, \end{aligned}$$

we can express the map P_0 corresponding to the Poincaré map as a map from G_0 back to itself by the concatenation of maps

$$P_0 : x \in G_0 \overset{\Phi_1}{\to} G_1 \overset{\Phi_1}{\to} G_1^\tau \overset{\Phi_2}{\to} G_2 \overset{\Phi_2}{\to} G_2^\tau \overset{\Phi_1}{\to} \ldots \overset{\Phi_2}{\to} G_m^\tau \overset{\Phi_1}{\to} G_0. \tag{16}$$

The symbol $G_k^\tau \overset{\Phi_j}{\to} G_{k+1}$ is defined as the map from a submanifold G_k^τ to a submanifold G_{k+1} obtained by following the flow Φ_j. All maps in (16) are well defined and smooth because the intersection of the flow Φ_j with the target manifold is always transversal due to Condition 6. For slowly oscillating orbits the reduction of the Poincaré map to P_0 is a well-established fact that has been used extensively in many studies of delayed relay systems, for example, in [24, 25, 26].

We remark that the map P_0 will, in general, be nonlinear, even if the local switching manifolds G_j and the flows Φ_1 and Φ_2 are affine, because the maps $G_j^\tau \mapsto G_{j+1}$ are nonlinear.

Furthermore, we remark that rapidly oscillating solutions (periodic orbits with $\mu > 0$ for all choices of Poincaré sections) can also occur as stable periodic orbits of a delayed relay system. Some of the periodic orbits found in [24, 25] have this structure. The rapidly oscillating orbits in the linearized pendulum discussed in section 4.1 are, however, all dynamically unstable [35].

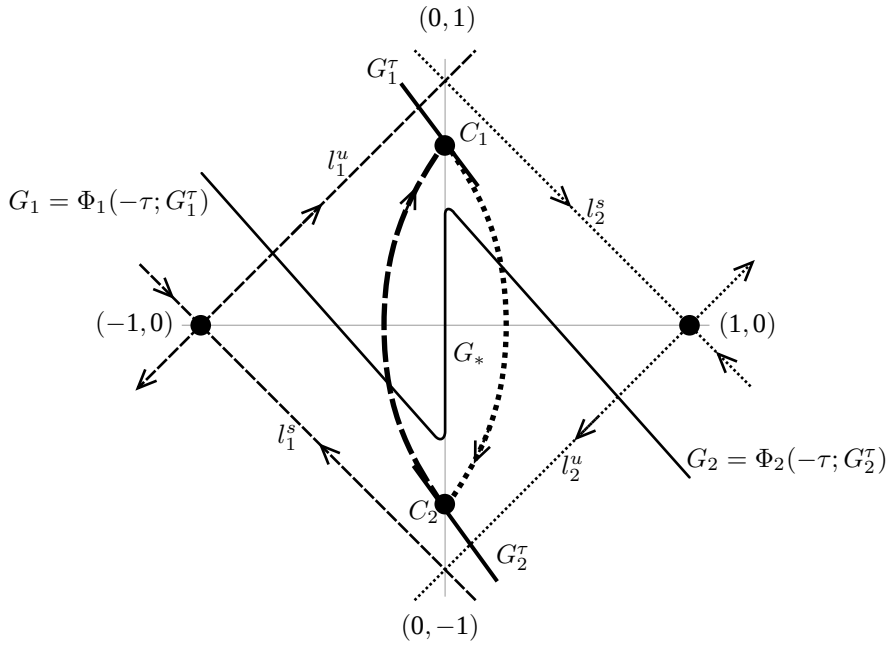

Figure 3. Construction of the switching line $G = G_1 \cup G_* \cup G_2$ and the stable periodic orbit $C_1 \to C_2 \to C_1$. For large delays τ, the lines G_1 and G_2 will be close to l_1^s and l_2^s, respectively. Trajectories of Φ_1 are dashed, trajectories of Φ_2 are dotted.

5. Existence of stable periodic orbits for arbitrarily large delay

Let us come back to Problem 1 formulated in the introduction and the resulting general Theorem 2 about the existence of stable periodic orbits. By choosing a suitable switching law g, we can create a periodic orbit resembling any closed curve in $\mathbb{R}^n$ that, in alternating fashion, follows Φ_1 and Φ_2, always for a time longer than the delay τ. Thus, this periodic orbit will be slowly oscillating, and its dynamical stability will be determined by the concatenation of $(n-1)$-dimensional maps of the form (16). Hence, we can achieve the dynamic stability of the periodic orbit by 'tilting' the local switching manifolds such that their time-τ images are tangential to desired hyperplanes.

5.1. Stabilization of the inverted pendulum

We first illustrate the main idea behind our construction of the desired switching function g for the inverted pendulum example. As mentioned in section 4.1, it is sufficient to find a function g, dividing $\mathbb{R}^2$ into two simple domains, such that the piecewise affine equation (8) has a stable periodic orbit for a given $\tau > 0$. More precisely, it is sufficient to construct the two domains, D_1 for the flow Φ_1 and D_2 for the flow Φ_2, and a smooth boundary G separating them. A smooth function g can then always be chosen such that clos $D_2 = \{g(x_1, x_2) \le 0\}$ and clos $D_2 = \{g(x_1, x_2) \ge 0\}$ (the notation clos refers to the closure of a set).

Figure 3 illustrates the following construction. First, we find a closed curve that consists of two segments, one following Φ_1, one following Φ_2, both for a time longer

than τ. Such a curve exists: the periodic orbit W found in section 4.1 is of this type if the points C_1 and C_2 are sufficiently close $(0, \pm 1)$, respectively. Let $h \in (0, 1/2)$ be such that

$$\mathrm{e}^\tau \in \left(h^{-1} - 1,\, h^{-1}\right). \tag{17}$$

If we choose $C_1 = (0, 2\mathrm{e}^\tau h - 1)^T$ and $C_2 = (0, 1 - 2\mathrm{e}^\tau h)$ then $\Phi_1(2\tau - \log(1-h^{-1}); C_2) = C_1$ and $\Phi_2(2\tau - \log(1-h^{-1}); C_1) = C_2$. The traveling time $2\tau - \log(1-h^{-1})$ is larger than τ by construction of h. Next, we find the boundary G such that this curve

$$W = \Phi_1([0, 2\tau - \log(1-h^{-1})]; C_2) \cup \Phi_2([0, 2\tau - \log(1-h^{-1})]; C_1) \tag{18}$$

is a stable periodic orbit of (8). The local delayed switching manifolds have to contain the corners: $C_1 \in G_1^\tau$ and $C_2 \in G_2^\tau$. If $G_1^\tau = C_1 + s\partial_1\Phi_2(0; C_1)$ where $s \in (-\delta, \delta)$ then G_1^τ is tangent to the outgoing flow Φ_2 in C_1. At the same time G_1^τ is transversal to the incoming flow Φ_1 in C_1. Thus, the image of G_1^τ under $\Phi_1(-\tau; \cdot)$ is an affine line segment G_1 intersecting W transversally within the (dashed) segment $\Phi_1([0, 2\tau - \log(1-h^{-1})]; C_2)$ of the curve W. The corresponding local manifolds for C_2 are $G_2^\tau = -G_1^\tau$ and $G_2 = -G_1$. Since W does not self-intersect we can connect G_1 and G_2 by a segment G_* and extend $G_1 \cup G_* \cup G_2$ to a global piecewise affine manifold G_0 which generates the periodic orbit W. This piecewise affine manifold can subsequently be smoothed at its corners (which have a positive distance to the curve W) to obtain a smooth switching manifold G; see Figure 3.

Lemma 8 *The periodic orbit W defined by (18) is stable.*

Proof: As demonstrated in section 4.1, the Poincaré map P for the periodic orbit W can be reduced to a one-dimensional return map P_0 from G_1^τ to itself, defined by following Φ_2 to G_2^τ and then Φ_1 back to G_1^τ. Let $p_0 = C_1 + s\partial_1\Phi_2(0; C_1)$ be a point in G_1^τ close to C_1 (that is, $s \in \mathbb{R}$ is small). Thus, $p_0 = \Phi_2(s; C_1) + \mathrm{O}(s^2)$. The traveling time $t(s)$ from p_0 to G_2^τ is $2\tau - \log(1-h^{-1}) - s + \mathrm{O}(s^2)$ for small s. Thus, the image of p_0 under the flow Φ_2 to G_2^τ is

$$p_0' = \Phi_2(t(s); \Phi_2(s; C_1)) = C_2 + \mathrm{O}(s^2).$$

Since the map defined by following Φ_1 from G_2^τ to G_1^τ is smooth this implies that $P_0(p_0) = C_1 + \mathrm{O}(s^2))$. □

We observe that the orbit W is even quadratically stable. That is, the linearization of P_0 in C_1 is zero. The periodic orbit W is also structurally stable. That is, it is robust with respect to small nonlinearities or small perturbations of the parameters, for example, of τ, or the location of the switching manifold. However, this tolerance is exponentially small for large τ since (17) gives effectively a condition on τ once h is chosen. Similarly, the basin of attraction of the periodic orbit W is exponentially small with respect to τ.

Remark 1: Apart from the fact that the relay stabilizes to a periodic orbit instead of the equilibrium, the exponential smallness of the basin of attraction is a difference to classical methods for delay compensation, such as finite spectrum assignment [29]. Finite spectrum assignment is a linear dynamic control law based on an explicit predictor. However, even though methods, such as finite spectrum assignment, are globally asymptotically stable on the linear level, they have exponentially large transients if the initial condition is not exponentially close to the equilibrium.

Remark 2: The study in [36] discusses systems of the form $\alpha\ddot{x}(t) = -\dot{x}(t) + kx(t) - \mathrm{sgn}x(t-1)$, finding conditions under which there are no bounded non-trivial oscillatory solutions. The crucial difference between [36] and the above construction, which gives a stable slowly oscillating solution for all $\alpha > 0$, $k > 0$ is that we allow the relay to depend not only on $x(t-1)$ but also on $\dot{x}(t-1)$. That is, the relay is of the form $\mathrm{sgn}g(x(t-1), \dot{x}(t-1))$, giving rise to a switching curve in figure 3 which is not vertical.

5.2. Stable periodic orbits in n-dimensional systems

As we have stated in Theorem 2 in the introduction, the construction of a relay switch for the simple two-dimensional inverted pendulum can be generalized to n-dimensional systems with saddle equilibria. The general piecewise smooth nonlinear system

$$\dot{y} = f(y, \varepsilon \operatorname{sgn} \tilde{g}(y(t-\tau))) \tag{19}$$

close to an equilibrium y_0 of $\dot{y} = f(y, 0)$ and for small ε can be rewritten as a perturbation of order ε of a piecewise affine system. Introducing the rescaled variable $x = \varepsilon^{-1}(y - y_0)$, the rescaled representation of the switching law $g(x) = \tilde{g}(y_0 + \varepsilon x)$, and the partial derivatives $A = \partial_1 f(y_0, 0)$, $v = -\partial_2 f(y_0, 0)$, the rescaled nonlinear system reads as

$$\dot{x} = Ax - v \operatorname{sgn} g(x(t-\tau)) + \varepsilon h(x, \operatorname{sgn} g(x(t-\tau)), \varepsilon) \tag{20}$$

where the function h is uniformly smooth for all ε near zero. Any stable periodic orbit $\tilde{x}(\cdot)$ found in the truncated system (20) with $\varepsilon = 0$ persists under small perturbations to the two vector fields (that is, to $\varepsilon > 0$). This implies the existence of a corresponding stable periodic orbit close to $\tilde{x}(\cdot)$ in (20) for sufficiently small $\varepsilon > 0$. Thus, (19) has a stable periodic orbit with an amplitude of order ε.

The pair (A, v) is called *controllable* if $(v, Av, \ldots, A^{n-1}v)$ has full rank n. An unbounded domain is called *simple* if its closure is homeomorphic to a half-space, say $\{z \in \mathbb{R}^n : z_1 \geq 0\}$. We call a periodic orbit W *quadratically stable* if

(i) it has a Poincaré map P which has a fixed point corresponding to W and is two times differentiable on the image of P^2 in a neighbourhood of its fixed point, and

(ii) the linearization of the Poincaré map in this fixed point is zero.

With these notations and arguments we can formulate a "linearized version" of Theorem 2, which, due to the above arguments, implies Theorem 2.

Theorem 9 *Let $A \in \mathbb{R}^{n,n}$ be a matrix that has eigenvalues with positive real part and eigenvalues with negative real part but no eigenvalues on the imaginary axis. Let $v \in \mathbb{R}^n$ be such that the pair (A, v) is controllable. Let $\tau > 0$ be arbitrary. Then there exists a smooth function $g : \mathbb{R}^n \to \mathbb{R}$ such that $\{z \in \mathbb{R}^n : g(z) = 0\}$ is a smooth manifold that splits $\mathbb{R}^n$ into two simple domains and such that the differential equation*

$$\dot{x}(t) = A\left[x(t) - v \operatorname{sgn} g(x(t-\tau))\right] \tag{21}$$

has a quadratically stable periodic orbit.

The spectral properties of A imply that, without the relay ($v = 0$), the origin is an equilibrium of saddle type. Moreover, they imply that the statement of Theorem 9 is equivalent to the corresponding statement for the truncated system (20) with $\varepsilon = 0$ because (A, v) is controllable if and only if $(A, A^{-1}v)$ is controllable.

The main difference between the n-dimensional case of Theorem 9 and the construction of W and G in section 5.1 is that the choice of G_j^τ tangential to

the outgoing flow eliminates only one dimension of the linearization. Thus, each switching at one of the delayed switching manifolds G_j^τ acts as a projection with a one-dimensional kernel on the linearization of P_0. This means that we have to find a closed curve Ψ consisting of an even number $m > n$ of segments Ψ_j, alternating between the two flows and always following each of the flows for a time θ_j greater than the delay τ. Subsequently, we have to verify that

(i) we can find a switching manifold that intersects each segment Ψ_j transversally exactly once in a point of our choice (namely, in $\Psi(\theta_j - \tau)$), and

(ii) we can tilt the switching manifold locally in the intersection points with Ψ in a manner such *that the concatenation of the projections induced by the switchings cancels out all components of the linearization.

The existence of an appropriate closed curve and point (i) follow from the saddle property of A, which implies that all trajectories that spend a long time near the equilibrium approximately follow first the stable and then the unstable subspace of A. The second point is implied by the controllability required in Theorem 9. The detailed proof of Theorem 9 is given in Appendix C.

6. Discontinuity-induced bifurcations

This section discusses what happens generically to the dynamics near relay periodic orbits that violate one of the transversality requirements, either Condition 5 or Condition 6. To simplify our presentation we restrict ourselves in this section to the practically most relevant case of slowly oscillating periodic orbits. We assume that the general delayed relay system (3) depends on a parameter λ where the dependence of f_1, f_2, g on x and λ and the dependence of τ on λ are smooth:

$$\dot{x}(t) = \begin{cases} f_1(x(t), \lambda) & \text{if } g(x(t - \tau(\lambda)), \lambda) < 0, \\ f_2(x(t), \lambda) & \text{if } g(x(t - \tau(\lambda)), \lambda) \geq 0. \end{cases} \tag{22}$$

Moreover, we assume that, for $\lambda < 0$, (22) has a slowly oscillating periodic orbit $\tilde{x}(\cdot, \lambda)$ of uniformly bounded period $p(\lambda)$, which satisfies the transversality conditions 5 and 6. Section 6.1 investigates the case of $\tilde{x}(\cdot, 0)$ violating Condition 5, section 6.2 studies the case of $\tilde{x}(\cdot, 0)$ violating Condition 6. This study treats (22) and the periodic orbit only at the parameter $\lambda = 0$. Thus, we can drop the parameter λ, which is always 0, from our notation in the remainder of the section.

6.1. Corner collision

The graph $\tilde{x}([-p, 0))$ of the periodic orbit is a continuous piecewise smooth curve in $\mathbb{R}^n$. The violation of Condition 5 means that one of the corners (switching points) of the curve $\tilde{x}([-p, 0))$ lies in the switching manifold $\{g = 0\}$. That is, at $\lambda = 0$ there are two times $\tilde{s}_1$ and $\tilde{s}_2$ such that

$$\tilde{s}_1 + \tau = \tilde{s}_2, \quad g(\tilde{x}(\tilde{s}_1)) = 0, \quad g(\tilde{x}(\tilde{s}_2)) = 0, \tag{23}$$

which violates Condition 5. The fact that $\tilde{x}(\cdot)$ is slowly oscillating for parameters $\lambda < 0$ implies that $\tilde{s}_1$ is the only intersection point of $\tilde{x}(\cdot)$ with $\{g = 0\}$ in the interval $[\tilde{s}_1 - \tau, \tilde{s}_2)$. Thus, $\tilde{x}(\cdot)$ follows exactly one flow in the time interval $[\tilde{s}_1, \tilde{s}_2]$ (say, Φ_1 without loss of generality).

We assume that $\tilde{x}$ satisfies the following two secondary non-degeneracy conditions:

Condition 10 (secondary genericity conditions for corner collision)

(a) Both vector fields intersect the switching manifold transversally in $\tilde{x}(\tilde{s}_2)$. That is, $g'(\tilde{x}(\tilde{s}_2))f_1(\tilde{x}(\tilde{s}_2)) \neq 0$, and $g'(\tilde{x}(\tilde{s}_2))f_2(\tilde{x}(\tilde{s}_2)) \neq 0$

(b) The local delayed switching manifold $G_1^\tau = \Phi_1(\tau; \{g = 0\}) \cap U(\tilde{x}(\tilde{s}_2))$ and the local switching manifold $G_2 = \{g = 0\} \cap U(\tilde{x}(\tilde{s}_2)))$ are not tangent to each other in $\tilde{x}(\tilde{s}_2)$. That is, $\partial_2\Phi_1(\tau; \tilde{x}(\tilde{s}_1))g'(\tilde{x}(\tilde{s}_1))^T$ and $g'(\tilde{x}(\tilde{s}_2))^T$ are linearly independent.

Let us choose as Poincaré section $\mathcal{S}$ the set of all $z \in C([-\tau, 0]; \mathbb{R}^n)$ with headpoint $z(0) \in G_1^\tau$. This is an admissible choice since G_1^τ intersects the incoming flow Φ_1 transversally.

Condition 10(b) implies that G_1^τ and G_2 intersect each other in the smooth local manifold $G_1^\tau \cap G_2$ of codimension 2, which contains $\tilde{x}(\tilde{s}_2)$. This intersection divides G_1^τ into two parts, $F_- := G_1^\tau \cap \{g < 0\}$ and $F_+ = G_1^\tau \cap \{g \geq 0\}$.

The following lemma states that the return map for $\tilde{x}$ can still be expressed as an $(n-1)$-dimensional return map P_0 to G_1^τ but that P_0 is only piecewise smooth with, in general, different derivatives in F_- and F_+.

Lemma 11 (Return map for corner collision) *The image of the local return map P of the periodic orbit $\tilde{x}(\cdot)$ is contained in a $(n-1)$-dimensional manifold that can be parametrized by the elements of G_1^τ. On G_1^τ, P is described by a piecewise smooth $(n-1)$-dimensional map P_0 which is smooth in F_+ and F_-. More precisely, there exist linear maps $A_1, A_2 \in \mathbb{R}^{n\times n}$ such that the local return map P_0 has the form*

$$P_0(\tilde{x}(\tilde{s}_2) + x) = \tilde{x}(\tilde{s}_2) + \begin{cases} A_1 x + O(\|x\|^2) & \text{if } \tilde{x}(\tilde{s}_2) + x \in F_-, \\ A_2 x + O(\|x\|^2) & \text{if } \tilde{x}(\tilde{s}_2) + x \in F_+ \end{cases} \tag{24}$$

for all sufficiently small $x \in G_1^\tau - \tilde{x}(\tilde{s}_2)$.

The first statement of Lemma 11 follows from the fact that all elements of $\mathcal{S}$ have an image under P of the form $\Phi_1([-\tau, 0]; z_0)$ where $z_0 \in G_1^\tau$. The piecewise linear asymptotics of P_0 comes, roughly speaking, from the fact that a trajectory through $\tilde{x}(\tilde{s}_2) + x \in F_+$ spends a different time in $\{g \geq 0\}$ than a trajectory through F_-. This time difference is asymptotically linear in x.

The precise dependence of A_1 and A_2 on the right-hand-side is described in Appendix D. There are three distinct cases (shown in a piecewise affine example in Figure 4), giving rise to different expressions for A_1 and A_2:

(a) $g'(\tilde{x}(\tilde{s}_2))f_1(\tilde{x}(\tilde{s}_2)) \cdot g'(\tilde{x}(\tilde{s}_2))f_2(\tilde{x}(\tilde{s}_2)) > 0$, shown in figure 4(a). This case corresponds to the situation where the periodic orbit $\tilde{x}$ intersects the switching manifold $\{g = 0\}$ transversally in $\tilde{x}(\tilde{s}_2)$ in the sense that all convex combinations $f_c = cf_1(\tilde{x}(\tilde{s}_2)) + (1-c)f_2(\tilde{x}(\tilde{s}_2))$ $(0 \leq c \leq 1)$ of the two tangent vectors at the corner satisfy $g'(\tilde{x}(\tilde{s}_2))f_c \neq 0$. That is, f_c points through the switching manifold for all $c \in [0, 1]$. Figure 4(a) illustrates this configuration where the periodic orbit intersects $\{g = 0\}$ at $\tilde{x}(\tilde{s}_2)$.

(b),(c) $g'(\tilde{x}(\tilde{s}_2))f_1(\tilde{x}(\tilde{s}_2)) \cdot g'(\tilde{x}(\tilde{s}_2))f_2(\tilde{x}(\tilde{s}_2)) < 0$. In both cases the periodic orbit lies (locally near $\tilde{x}(\tilde{s}_2)$) entirely on one side of the switching manifold. This implies that $\tilde{x}(\cdot)$ intersects (touches) the switching manifold an odd number of times. The form of A_1 and A_2 depends also on the existence of another intersection $\tilde{x}(\tilde{s}_3)$ of the periodic orbit $\tilde{x}(\cdot)$ with the switching manifold $\{g = 0\}$ within in the interval $(\tilde{s}_2, \tilde{t}_2)$ where $\tilde{t}_2 = \tilde{s}_2 + \tau$. The difference between the cases (b) and (c), shown in figure 4(b) and (c), is the order of $\tilde{x}(\tilde{s}_3)$ and $\tilde{x}(\tilde{t}_2)$ along the orbit $\tilde{x}$. The effect of

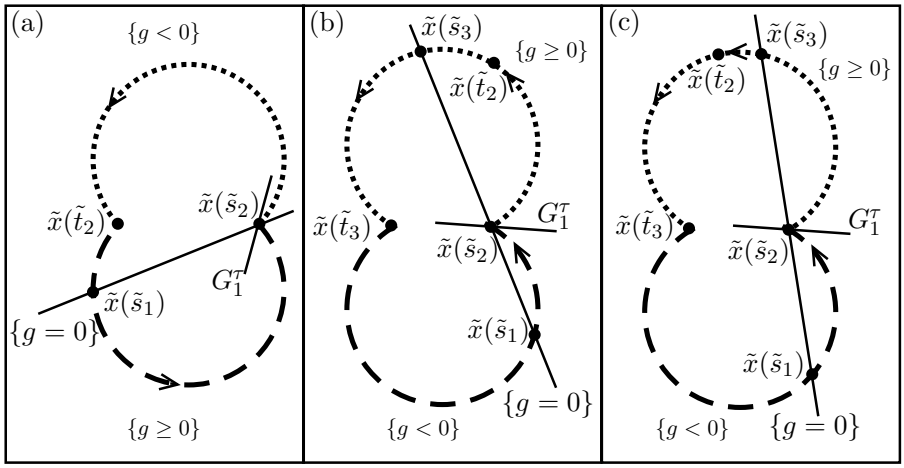

Figure 4. Illustration of a periodic orbit $\tilde{x}$ undergoing a corner collision at $\tilde{x}(\tilde{s}_2)$, showing the three different possible configurations. The times $\tilde{s}_j$ $(j=1,2,3)$ are the moments when $\tilde{x}$ intersects the switching manifold $\{g=0\}$. The times $\tilde{t}_j$ are the corresponding switching times ($\tilde{t}_j=\tilde{s}_j+\tau$, $\tilde{t}_1=\tilde{s}_2$). The manifold G_1^τ is the time-τ image of $\{g=0\}$ under Φ_1. The return map P_0, discussed in Lemma 11, maps the local manifold G_1^τ back to itself. The dashed part of $\tilde{x}$ follows Φ_1, the dotted part follows Φ_2.

this difference on the dynamics becomes clear if both flows are linearly dependent in the delayed switching point $\tilde{x}(\tilde{t}_2)$ (that is, $f_1(\tilde{x}(\tilde{t}_2))$ and $f_2(\tilde{x}(\tilde{t}_2))$ are linearly dependent). Then the linearization of the return map will be continuous for case (b) but, in general, it will still be discontinuous for case (c). Case (c) is the most complex scenario because the discontinuity is affected by the configuration at four different points along the orbit: at $\tilde{x}(\tilde{s}_2)$, $\tilde{x}(\tilde{s}_3)$, $\tilde{x}(\tilde{t}_2)$, and $\tilde{x}(\tilde{t}_3)$.

The dynamics of piecewise asymptotically linear maps have been studied in [13, 14], also classifying possible bifurcations when the parameter λ unfolds the degeneracy transversally. Thus, Lemma 11 links the study of the infinite-dimensional delayed relay system to the bifurcation theory of piecewise smooth asymptotically linear finite-dimensional maps.

6.2. Tangential grazing

The violation of Condition 6 means that there exists a time s_* when the periodic orbit grazes (touches) the switching manifold $\{g=0\}$ tangentially, that is, $g(\tilde{x}(s_*))=0$ and $g'(\tilde{x}(s_*))\dot{\tilde{x}}(s_*)=0$. Let us denote the transversal switching times along $\tilde{x}$ by $\tilde{s}_j$ $(j=1,\dots,m$ where m is even). We assume that $\tilde{x}(\cdot)$ satisfies the following secondary non-degeneracy conditions:

Condition 12 (secondary genericity conditions for tangential grazing)

(a) The orbit $\tilde{x}$ is quadratically tangent to the switching manifold $\{g=0\}$ in s_*, and not to a higher order. That is,

$$q:=\frac{1}{2}\frac{d^2}{[dt]^2}g(\tilde{x}(t))\big|_{t=s_*}=\frac{1}{2}\left[g'(\tilde{x}(s_*))\ddot{\tilde{x}}(s_*)+g''(\tilde{x}(s_*))\left[\dot{\tilde{x}}(s_*)\right]^2\right]\neq 0.$$

(b) The time when the tangency is noticed along the orbit $\tilde{x}$ does not coincide with another crossing of the switching manifold. That is, $g(\tilde{x}(t_*)) \neq 0$ where $t_* = s_* + \tau$.

(c) The grazing does not coincide with a simultaneous violation of Condition 5 (a corner collision). That is, $g(\tilde{x}(s_* - \tau)) \neq 0$. Hence, $s_* \neq \tilde{t}_j$ $(j = 1, \ldots, m)$ where $\tilde{t}_j = \tilde{s}_j + \tau$.

The periodic orbit $\tilde{x}$ is slowly oscillating for parameter $\lambda < 0$. Thus, s_* lies in an interval $[a, b]$ which is longer than the delay τ (that is, $b - a > \tau$) where $\tilde{x}$ follows one flow. Without loss of generality, let us assume that $\tilde{x}([a, b])$ follows Φ_1. We choose as Poincaré section $\mathcal{S}$ the set of all $z \in C([-\tau, 0]; \mathbb{R}^n)$ with headpoint $z(0) \in G$ where G is a hyperplane intersecting $\tilde{x}$ transversally at time $\tilde{t}_0 = (a + b + \tau)/2$. The following lemma describes the local return map P to the Poincaré section $\mathcal{S}$ to leading order.

Lemma 13 (Return map for tangential grazing) *The image of the local return map P to the Poincaré section $\mathcal{S}$ is contained in a $(n-1)$-dimensional manifold that can be parametrized by the elements of the affine hyperplane*

$$F_0 := \{x : \dot{\tilde{x}}(s_*)^T [x - \tilde{x}(s_*)] = 0\}.$$

On F_0, P is described by a piecewise smooth $(n-1)$-dimensional map $P_0 : F_0 \mapsto F_0$. There exists a smooth function $m : U(\tilde{x}(s_*)) \to \mathbb{R}$ such that the map P_0 is smooth in $F_+ = F_0 \cap \{x : m(x) > 0\}$ and $F_- = F_0 \cap \{x : m(x) < 0\}$. For small $x \in F_0 - \tilde{x}(s_*)$ the map P_0 has the form

$$P_0(\tilde{x}(s_*) + x) = \tilde{x}(s_*) + \begin{cases} Ax + \mathrm{O}(\|x\|^2) & \text{if } \tilde{x}(s_*) + x \in F_+, \\ v\sqrt{-m(\tilde{x}(s_*) + x)} + \mathrm{O}(\|x\|) & \text{if } \tilde{x}(s_*) + x \in F_- \end{cases} \tag{25}$$

where $A \in \mathbb{R}^{n \times n}$ and $v \in F_0 - \tilde{x}(s_*) \subset \mathbb{R}^n$.

The expansion of the function m in $\tilde{x}(s_*)$ is

$$m(\tilde{x}(s_*) + x) = q^{-1} g'(\tilde{x}(s_*))x + \mathrm{O}(\|x\|^2).$$

This implies that the return map of all trajectories near $\tilde{x}(\cdot)$ that intersect F_- expands to lowest order like a square root. The first statement of Lemma 13 follows from the fact that all elements of $\mathcal{S}$ will have an image under P which has the form $\Phi_1([-\tau, 0]; z_0)$ where $z_0 \in G$. This reduces the Poincaré map P to a return map to the hyperplane $G \subset \mathbb{R}^n$. Since both hyperplanes F and G are transversal to $\tilde{x}$, return maps to G and to F are conjugate to each other under the local diffeomorphism obtained by following the flow Φ_1 from F to G.

The function $m(x)$ used in Lemma 13 is defined as the local minimum of the parabola-shaped function $q^{-1} g(\Phi_1(\cdot; x))$ near 0. This local minimum is uniquely defined and depends smoothly on x. The square-root asymptotics of P_0 arises, roughly speaking, from the fact that the time which a trajectory through $\tilde{x}(\tilde{s}_2) + x \in F_-$ spends in $\{x : m(x) < 0\}$ depends asymptotically linearly on the square root of $-m(x)$.

The precise dependence of A and v on the right-hand-side is described in detail in Appendix E. Figure 5 illustrates the two different cases that can arise. The difference between the two cases is that in case (a) $\tilde{x}$ does not cross the switching manifold $\{g = 0\}$ between s_* and t_*, whereas in case (b) there is an intermediate crossing at $\tilde{x}(\tilde{s}_2)$. Both cases have two sub-cases depending on the existence of the intermediate switching at $\tilde{t}_1$ between s_* and t_*, but those cause only minor differences. Case (b) is more complex because the discontinuity of the return map is affected by the

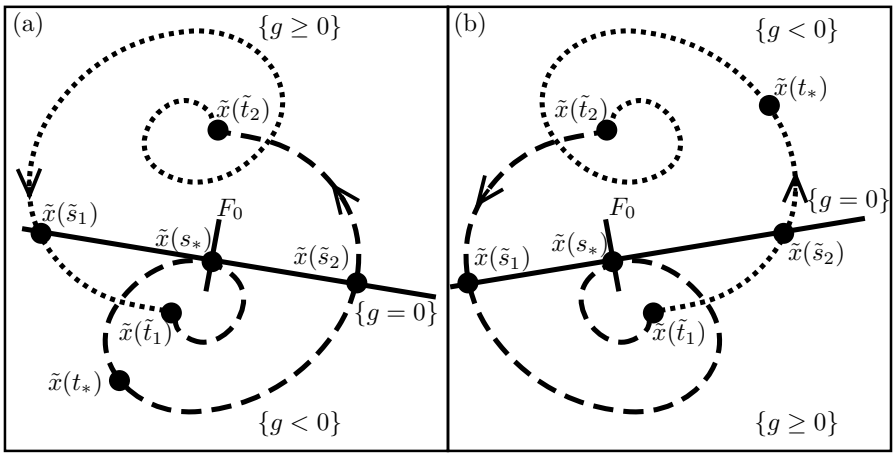

Figure 5. Illustration of a periodic orbit $\tilde{x}$ undergoing a tangential grazing at $\tilde{x}(s_*)$, showing the two different possible configurations. The times $\tilde{s}_j$ $(j = 1, 2)$ are the moments when $\tilde{x}$ intersects the switching manifold $\{g = 0\}$ transversally. The times $\tilde{t}_j$ are the corresponding switching times ($\tilde{t}_j = \tilde{s}_j + \tau$). At the point $\tilde{x}(t_*)$ the system notices the grazing at s_*. The return map P_0, discussed in Lemma 13, maps the local manifold F_0 (defined as being orthogonal to $\dot{\tilde{x}}(s_*)$) back to itself. The dashed part of $\tilde{x}$ follows Φ_1, the dotted part follows Φ_2.

configurations near four points along the periodic orbit: $\tilde{x}(s_*)$, $\tilde{x}(\tilde{s}_2)$, $\tilde{x}(t_*)$ and $\tilde{x}(\tilde{t}_2)$. A special case of type (a) is a periodic orbit of period larger than the delay τ that has no transversal intersections with the switching manifold $\{g = 0\}$.

Lemma 13 allows one to link phenomena occurring close to a grazing periodic orbit in a delayed relay system to the bifurcation theory of piecewise smooth maps with square-root asymptotics on one side of the discontinuity. The general results in [15, 16] classify the dynamics for maps of this type.

6.3. The dynamics near grazing bifurcations in the small-delay limit — illustrating example

The occurrence of square-root terms in return maps as in Lemma 13 is typical for impacting systems in the vicinity of periodic orbits with slow-velocity impacts rather than ordinary differential equations with discontinuous right-hand-side (that is, systems such as (3) with $\tau = 0$, so-called Filippov systems [14]). A consequence of this fact is that the dynamics of system (3) can change dramatically by changing τ from 0 to a small positive value. The reason behind this change is that codimension-one grazing events of periodic orbits generically induce C^1-smooth or piecewise asymptotically linear return maps for Filippov systems, in contrast to impacting systems, or the case of (3) with a positive delay. As an illustrative example we consider the system in $\mathbb{R}^2$

$$\dot{x} = \begin{cases} \begin{bmatrix} 0 & -1 \\ 1 & 0 \end{bmatrix} x - a \cdot (\|x\| - \lambda) & \text{if } x_1(t-\tau) - 1 < 0, \\ f_2(x) & \text{if } x_1(t-\tau) - 1 \geq 0 \end{cases} \tag{26}$$

where $a > 0$, $\lambda > 0$, $\|\cdot\|$ is the Euclidean norm in $\mathbb{R}^2$, and $f_2(x_0) = (-b, 0)$ at $x_0 = (1, 0)$ with $b > 0$. The switching function g is $g(x) = x_1 - 1$. This system

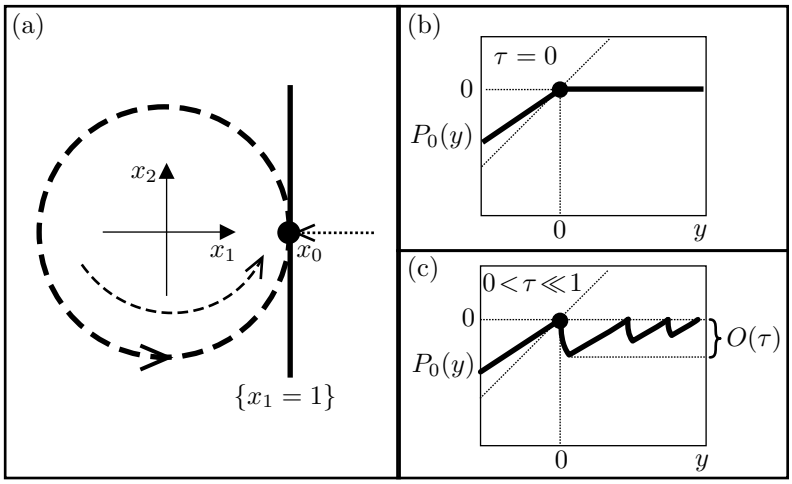

Figure 6. Illustration of the configuration for the periodic orbit of (26). Panel (a) shows the phase portrait for the grazing periodic orbit. The dashed trajectories correspond to flow Φ_1 with its stable limit cycle, the dotted arrow shows $f_2(x_0)$. Panels (b) and (c) show the asymptotics of the local return map P_0 to $\{x_2 = 0\}$ for $y = x_1 - 1$ for small y, and delay $\tau = 0$ (b) or small delay (c).

has a stable limit cycle $(\tilde{x}_1(t), \tilde{x}_2(t)) = (\lambda\cos(t), \lambda\sin(t))$ if $\lambda < \lambda_0 = 1$. At the parameter value $\lambda = 1$ the periodic orbit $\tilde{x}(\cdot)$ grazes tangentially the switching line $\{x_1 = 1\}$ in x_0. Figure 6 illustrates this situation in panel (a). For $\tau = 0$ the orbit continues to exist also for $\lambda \geq 1$ ($\lambda \approx 1$), changes its shape continuously and remains stable. In fact, for $1 < \lambda \ll 2$ the orbit slides along the line $\{x_1 = 1\}$ from $x_2 = -\sqrt{\lambda^2 - 1}$ to $x_2 = \sqrt{\lambda^2 - 1}$ (due to $f_2(x_0)$ pointing toward the sliding line in the grazing point). Thus, at the grazing its only non-trivial Floquet multiplier jumps from $c = \exp(-4\pi a) \in (0, 1)$ for $\lambda < 1$ to 0 for $\lambda > 1$.

If, however, τ is small but positive the return map P_0 to the line segment $x_2 = 0$, $x_1 \in [1 - \delta, 1 + \delta]$ has the form described in Lemma 13 for $\lambda = 1$. Specifically, introducing the variable $y = x_1 - 1$,

$$P_0(y) = \begin{cases} cy & \text{if } y < 0 \\ -d\sqrt{y} + \mathrm{O}(|y|) & \text{if } 0 \leq y \ll 1 \end{cases} \tag{27}$$

where d is a positive factor close to $2bc$. The Poincaré map of the grazing periodic orbit is depicted in figure 6(c), comparing it to the return map without delay in panel (b). The expression in (27) captures only the first square root branch of the return map of height $\mathrm{O}(\tau)$. The dynamics of maps with square-root asymptotics has been studied by [15, 16]. A consequence of the results of [16] is that, if $\exp(-4\pi a) > 2/3$, for any given $\tau > 0$ the system has a chaotic attractor for all λ in an interval $(1, \lambda_{\max}(\tau))$. This sudden transition to chaos by an introduction of an arbitrarily small delay is fundamentally different from the behaviour of smooth systems. If one introduces a small delay in one of the arguments of a smooth system of ODEs the delay acts as a regular perturbation parameter, preserving, for example, hyperbolic equilibria or periodic orbits without changing their stability [37].

7. Conclusion

The paper considered the dynamics of dynamical systems with delayed relays in the vicinity of periodic orbits. First, we found that the dynamics can be described generically by low-dimensional local return maps, even though the phase space of the original system is infinite-dimensional. Generically these return maps are smooth. Specifically, we provided two sufficient genericity conditions on the periodic orbit that guarantee the smoothness and finite-dimensionality of the local return map.

We exploited the existence and form of these local return maps to show that relays can be used to design simple static feedback laws that are able to stabilize saddle-type equilibria to nearby periodic orbits even in the presence of arbitrarily large delays.

Finally, we studied the two most common bifurcations that occur when one of the genericity conditions is violated: the corner collision and the tangential grazing. They give rise to piecewise smooth local return maps. These return maps are either piecewise asymptotically linear (corner collision) or have square-root asymptotics on one side (grazing). The reduction to piecewise smooth maps provides a link to well-established results of the bifurcation theory for these types of maps [13, 14, 15, 16]. It also shows that the small-delay limit for relay systems is more subtle than the corresponding limit for smooth DDEs.

The main open problem concerning the bifurcation theoretic part of our studies is that the secondary non-degeneracy conditions, even though they are genericity conditions, are often not fulfilled in practice. Typically, symmetric periodic orbits of piecewise linear systems of the form $\dot{x} = Ax - v\mathrm{sgn}[b^T x(t-\tau)]$ violate the secondary non-degeneracy conditions formulated in the sections 6.1 and 6.2 whenever they violate the primary conditions 5 or 6. This gives rise to much more degenerate bifurcation scenarios in the systems studied in [24, 25].

A caveat of the stabilizability result in Theorem 9 is that the basin of attraction of the quadratically stable periodic orbit shrinks not only for increasing τ but also for decreasing amplitude of the orbit (which is related to the size of ε). A possible solution to this problem are the more general hybrid feedback control law. For example, a hybrid feedback for the inverted pendulum would give rise to a dynamical system of the form

$$\ddot{x} = x - \alpha \quad \text{where } \alpha = \begin{cases} 1 & \text{if } x(t-\tau) \in D_+, \\ 0 & \text{if } x(t-\tau) \in D_0, \\ -1 & \text{if } x(t-\tau) \in D_-, \end{cases}$$

where $D_+ \cup D_0 \cup D_-$ is a partition of the physical space $\mathbb{R}^n$. This type of hybrid control could potentially allow one to decrease the amplitude of the periodic motion without shrinking its basin of attraction. Moreover, one can choose this partition such that the time spent in D_0 by the periodic orbit is arbitrarily close to p, the period of the orbit. This means that the relay control could be switched off most of the time.

Another limitation of the stabilizability result in Theorem 9 is its restriction to matrices of saddle-type. A modification of the arguments given in the illustration in section 5.1 and the general proof in Appendix C enables one to extend the result to completely unstable matrices in certain cases (for example, the case of a matrix with two different real positive eigenvectors).

Acknowledgments

The research of J.S. is supported by EPSRC grant GR/R72020/01. The author thanks his colleagues Bernd Krauskopf, Piotr Kowalczyk and David Barton for fruitful discussions and, in particular, Bernd Krauskopf for his help on improving the presentation of the material.

[1] M. Garcia, A. Chatterjee, and A. Ruina. Efficiency, speed, and scaling of passive dynamical bipedal walking. *Dynamics and Stability of Systems*, 15(2):75–99, 2000.
[2] F. Moss and J.G. Milton. Balancing the unbalanced. *Nature*, 425:911–912, 2003.
[3] H. Kwakernaak and R. Sivan. *Linear Optimal Control Systems*. Wiley Interscience, New York, 1972.
[4] G. Stépán. *Retarded Dynamical Systems*: *Stability and Characteristic Functions*. Longman Scientific and Technical, 1989.
[5] F.M. Atay. Balancing the inverted pendulum using position feedback. *Appl. Math. Letters*, 12:51–56, 1999.
[6] J. Sieber and B. Krauskopf. Extending the permissible control loop latency for the controlled inverted pendulum. *Dynamical Systems*: *An International Journal*, 20(2):189–199, 2005.
[7] W. Michiels and D. Roose. Limitations of delayed state feedback: a numerical study. *International Journal of Bifurcation and Chaos*, 12(6):1309–1320, 2002.
[8] M. Landry, S.A. Campbell, K. Morris, and C. Aguilar. Dynamics of an inverted pendulum with delayed feedback control. Preprint, University of Waterloo, 2003. submitted.
[9] J. Sieber and B. Krauskopf. Bifurcation analysis of an inverted pendulum with delayed feedback control near a triple-zero eigenvalue. *Nonlinearity*, 17(1):85–104, 2004.
[10] L. Fridman, E. Fridman, and E. Shustin. Steady modes and sliding modes in relay control systems with delay. In J. P. Barbot and W. Perruguetti, editors, *Sliding Mode Control in Engineering*, pages 264–295. New York, 2002.
[11] L. Fridman, V. Strygin, and A. Polyakov. Stabilization of amplitude of oscillations via relay delay control. *Int. J. Control*, 76(8):770–780, 2003.
[12] O. Diekmann, S. van Gils, S.M. Verduyn Lunel, and H.-O. Walther. *Delay Equations*, volume 110 of *Applied Mathematical Sciences*. Springer-Verlag, 1995.
[13] S. Banerjee and C. Grebogi. Border collision bifurcations in twodimensional piecewise smooth maps. *Phys. Rev. E*, 59:4052–4061, 1999.
[14] M. di Bernardo, M.I. Feigin, S.J. Hogan, and M.E. Homer. Local analysis of C-bifurcations in n-dimensional piecewise smooth dynamical systems. *Chaos, Solitons and Fractals*, 10:1881–1908, 1999.
[15] A.B. Nordmark. Universal limit mapping in grazing bifurcations. *Phys. Rev. E*, 55:266–270, 1997.
[16] H. Nusse, E. Ott, and J. Yorke. Border collision bifurcations: an explanation for observed bifurcation phenomena. *Phys. Rev. E*, 49:1073–1076, 1994.
[17] J. Gonçalves, A. Megretzki, and M.A. Dahleh. Global stability of relay feedback systems. *IEEE Transactions on Automatic Control*, 46(4):550–562, 2001.
[18] K.H. Johansson, A.E. Barabanov, and K.J. Åström. Limit cycles with chattering in relay feedback systems. *IEEE Transaction on Automatic Control*, 47(9):1414–1423, 2002.
[19] K. Popp and P. Stelter. Stick-slip vibrations and chaos. *Philosophical Transactions*: *Physical Sciences and Engineering*, 332(1624):89–105, 2000.
[20] B. Brogliato. *Impacts in mechanical systems — analysis and modelling*, volume 551 of *Lecture notes in physics*. Springer-Verlag, 2000.
[21] S. Banerjee and G.C. Verghese. *Nonlinear phenomena in power electronics*: *attractors, bifurcations, chaos, and nonlinear control*. IEEE Press, New York, 2001.
[22] J.-L. Gouzé and T. Sari. A class of piecewise linear differential equations arising in biological models. *Dynamical systems*, 17:299–316, 2003.
[23] D.A.W. Barton, B. Krauskopf, and R.E. Wilson. Explicit periodic solutions in a model of a relay controller with delay and forcing. *Nonlinearity*, 18(6):2637–2656, 2005.
[24] D.A.W. Barton, B. Krauskopf, and R.E. Wilson. Periodic solutions and their bifurcations in a non-smooth second-order delay differential equation. Preprint 2005.15, University of Bristol, Bristol Centre for Applied Nonlinear Mathematics, 2005. `http://www.enm.bris.ac.uk/anm/preprints/2005r15.html`.
[25] W. Bayer and U. an der Heyden. Oscillation types and bifurcations of a nonlinear second-order differential-difference equation. *J. Dynam. Diff. Eq.*, 10(2):303–326, 1998.

[26] U. Holmberg. *Relay feedback of simple systems*. PhD thesis, Lund Institute of Technology, 1991.
[27] H.-O. Walther. Contracting return maps for monotone delayed feedback. *Discrete and Continuous Dynamical Systems*, 7(2):259–274, 2001.
[28] Y.-H. Roh and J.-H. Oh. Robust stabilization of uncertain input-delay systems by sliding mode control with delay compensation. *Automatica*, 35:1861–1865, 1999.
[29] Q.G. Wang, T.H. Lee, and K.K. Tan. Finite spectrum assignment for time-delay systems. In *Lecture notes in control and information sciences*, volume 239. Springer Verlag, New York, 1999.
[30] S. Mondié and W. Michiels. Finite spectrum assignment of unstable time-delay systems with a safe implementation. *IEEE Transactions on Automatic Control*, 48(12):2207–2212, 2003.
[31] T. Horiuchi and T. Konno. A new method for compensating actuator delay in real-time hybrid experiments. *Philosophical Transactions of the Royal Society A*, 359:1893–1909, 2001.
[32] M.I. Wallace, D.J. Wagg, and S.A. Neild. An adaptive polynomial based forward prediction algorithm for multi-actuator real-time dynamic substructuring. Accepted for publication in Proceedings of the Royal Society of London A.
[33] J.K. Hale and S.M. Verduyn Lunel. *Introduction to Functional Differential Equations*, volume 99 of *Applied Mathematical Sciences*. Springer-Verlag, 1993.
[34] A. Pazy. *Semigroups of Linear Operators and Applications to Partial Differential Equations*. Applied mathematical Sciences. Springer Verlag, New York, 1983.
[35] J. Sieber. Dynamics of delayed relay control systems with large delays. In *Proceedings of the 5th IFAC Workshop on Time-Delay Systems, Leuven, Belgium*, 2004.
[36] E. Shustin, E. Fridman, and L. Fridman. Stable oscillations in a discontinuous delay system of the second order. *Discrete Contin. Dynam. Systems*, (Added Volume II):209–233, 1998. Dynamical systems and differential equations, Vol. II (Springfield, MO, 1996).
[37] C. Chicone. Inertial and slow manifolds for delay equations with small delays. *Journal of Differential Equations*, 190:364–406, 2003.

Appendix A. Proof of Lemma 4

It is sufficient to prove the continuity of $E(T;\cdot)$ in $\tilde{x}_{t_0}$ for $T \in (0,\tau)$ since $\tilde{x}_{t_0}$ lies on a periodic orbit. The set of all roots of $g(\tilde{x}_{t_0}(\theta))$ within $[-\tau,-\tau+T]$ is a subset of $\{t_0+\tilde{s}_1,\ldots,t_0+\tilde{s}_m\}$. Let us denote these time points by r_j $(j=1,\ldots,q,\ q\le m)$ in ascending order: $-\tau \le r_1 < \ldots < r_q \le T-\tau$. We define the constant

$$C = \max_{\theta\in\mathbb{R}} \left[\|f_1(\tilde{x}(\theta))\| + \|f_2(\tilde{x}(\theta))\|\right]$$

which is bounded since $\tilde{x}$ is periodic and the functions f_j are Lipschitz continuous. Let $\varepsilon > 0$ be small enough such that $\exp(4\varepsilon L) < 2$ where L is a Lipschitz constant for f_1 and f_2. In order to prove continuity it is sufficient to find a $\delta > 0$ such that

$$\|E(T;\xi) - E(T;\tilde{x}_{t_0})\| < (8C+1)\left(2\mathrm{e}^{LT}\right)^{q+1}\varepsilon \tag{A.1}$$

for all $\xi \in C([-\tau,0];\mathbb{R}^n)$ satisfying $\|\xi - \tilde{x}_{t_0}\| < \delta$ in the (maximum) norm of $C([-\tau,0];\mathbb{R}^n)$. We choose $\delta \in (0,\varepsilon)$ such that all $\xi \in C([-\tau,0];\mathbb{R}^n)$ with $\|\xi-\tilde{x}_{t_0}\| < \delta$ meet the following condition: $g(\xi(\theta))$ is nonzero and has the same sign as $g(\tilde{x}_{t_0}(\theta))$ for all $\theta \in [-\tau,T-\tau] \setminus \bigcup_{j=1}^{q}(r_j-\varepsilon, r_j+\varepsilon)$. That is, for all ξ in the δ-neighbourhood of $\tilde{x}_{t_0}$, $g(\xi(\cdot))$ can have zeroes only in the vicinity of the zeroes of $g(\tilde{x}_{t_0}(\cdot))$.

Let $\xi \in C([-\tau,0];\mathbb{R}^n)$ be such that $\|\xi-\tilde{x}_{t_0}\| < \delta$. Since $E(T;\cdot)(\theta) = E(0;\cdot)(\theta+T)$ for $\theta \in [-\tau,-T]$, we have

$$\|E(T;\xi)(\theta) - E(T;\tilde{x}_{t_0})(\theta)\| < \delta < \varepsilon \quad \text{for } \theta \in [-\tau,-T]. \tag{A.2}$$

If $\theta \in (-T,0]$ then $E(T;\cdot)(\theta) = E(\theta+T;\cdot)(0)$. Consequently, we have to focus on the evolution of the difference between the headpoints, $x(t) := E(t;\xi)(0)$ and $\tilde{x}(t_0+t)$, $\Delta(t) := \|x(t) - \tilde{x}(t_0+t)\|$, for $t \in [0,T]$. Inequality (A.2) implies that $|\Delta(0)| < \varepsilon$. If t is not in $\bigcup_{j=1}^{q}(\tau+r_j-\varepsilon, \tau+r_j+\varepsilon)$ then both headpoints follow the same flow (either

Φ_1 or Φ_2). Thus, we have the following set of recursive inequalities for the evolution of $\Delta(t)$ in the intervals $(\tau + r_j + \varepsilon, \tau + r_{j+1} - \varepsilon)$:

$$\begin{aligned}
\Delta(t) &< \mathrm{e}^{Lt}\Delta(0) < \mathrm{e}^{LT}\varepsilon \qquad \text{if } 0 \le t \le \tau + r_1 - \varepsilon, \\
\Delta(t) &< \mathrm{e}^{L(t-(\tau+r_j+\varepsilon))}\Delta(\tau + r_j + \varepsilon) \\
&< \mathrm{e}^{LT}\Delta(\tau + r_j + \varepsilon) \quad \text{if } \tau + r_j + \varepsilon \le t \le \tau + r_{j+1} - \varepsilon \ (j = 1, \dots, q-1), \\
\Delta(t) &< \mathrm{e}^{L(t-(\tau+r_q+\varepsilon))}\Delta(\tau + r_q + \varepsilon) \\
&< \mathrm{e}^{LT}\Delta(\tau + r_q + \varepsilon) \quad \text{if } \tau + r_q + \varepsilon \le t \le T.
\end{aligned} \tag{A.3}$$

The variation-of-constants formula (7) implies an estimate on how $\Delta(t)$ evolves in the intervals $(\tau + r_j - \varepsilon, \tau + r_j + \varepsilon)$. Let t_1, t_2 be in $[0, T] \cap (\tau + r_j - \varepsilon, \tau + r_j + \varepsilon)$ for some j and $t_1 < t_2$:

$$\begin{aligned}
\Delta(t_2) \le\ & \Delta(t_1) + \|x(t_2) - x(t_1)\| + \|x_{t_0}(t_2) - x_{t_0}(t_1)\| \\
&\le \Delta(t_1) + \int_{t_1}^{t_2} \|f_1(x(s))\| + \|f_2(x(s))\| ds + \\
&\qquad + \int_{t_1}^{t_2} \|f_1(x_{t_0}(s))\| + \|f_2(x_{t_0}(s))\| ds \\
&\le \Delta(t_1) + 2\int_{t_1}^{t_2} \|f_1(x_{t_0}(s))\| + \|f_2(x_{t_0}(s))\| ds + 2L\int_{t_1}^{t_2} \Delta(s) ds \\
&\le \Delta(t_1) + 2(t_2 - t_1)C + 2L\int_{t_1}^{t_2} \Delta(s) ds \\
&\le [\Delta(t_1) + 2C(t_2 - t_1)]\, \mathrm{e}^{2L(t_2 - t_1)} \\
&\le 2\Delta(t_1) + 4C(t_2 - t_1)
\end{aligned} \tag{A.4}$$

The recursion of inequalities (A.3) and estimate (A.4) (where always $t_2 - t_1 < 2\varepsilon$) allow for a global estimate of $\Delta(t)$ for $t \in [0, T]$:

$$\begin{aligned}
\Delta(t) \le\ & \mathrm{e}^{LT}\left[8C + 8C\,2\mathrm{e}^{LT} + \ldots + 8C(2\mathrm{e}^{LT})^{q-1} + (2\mathrm{e}^{LT})^q\right]\varepsilon \\
\le\ & (8C + 1)\left(2\mathrm{e}^{LT}\right)^{q+1}\varepsilon
\end{aligned} \tag{A.5}$$

The inequalities (A.2) and (A.5) combined imply the validity of the estimate (A.1) for the whole maximum norm of the function $E(T; x) - E(T; x_{t_0})$. □

Appendix B. Proof of Lemma 7

Let $\delta > 0$ be such that all intervals $(-p, -p + \delta)$, $(\tilde{s}_k - \delta, \tilde{s}_k + \delta)$, $(\tilde{t}_k - \delta, \tilde{t}_k + \delta)$ and $(-\delta, 0)$ are disjoint $(k = 1, \dots, m)$. This is possible due to Condition 5 on $\tilde{x}$.

Let $\tilde{s}_k$ $(k \in \{1, \dots, m\})$ be one of the zeroes of $g(\tilde{x}(\cdot))$ in $(-p, 0)$. Due to Condition 5 the periodic orbit $\tilde{x}$ follows one of the flows in $\tilde{s}_k$, say Φ_j. Because of the transversality of Φ_j with $\{g = 0\}$ in $\tilde{x}(\tilde{s}_k)$ (Condition 6) there exists a $\varepsilon_k > 0$ such that the function $t \to g(\Phi_j(t; z))$ changes its sign and has exactly one zero in $(-\delta, \delta)$ for all $z \in \mathbb{R}^n$ with $\|z - \tilde{x}(\tilde{s}_k)\| < \varepsilon_k$. Furthermore, for sufficiently small δ there exists a ε_0 such that the function $t \to l_0^T[\Phi_1(t; z) - \tilde{x}(0)]$ has exactly one regular zero in $(-\delta, \delta)$ for all $z \in \mathbb{R}^n$ with $\|z - \tilde{x}(0)\| < \varepsilon_0$. We define $\varepsilon := \min\{\varepsilon_k : k = 0 \dots, m\}$, which is larger than zero.

Let the open neighbourhood $\mathcal{N} \subset \mathcal{S}$ of $\tilde{x}_0$ be sufficiently small such that for all $\xi \in \mathcal{N}$ the following three Conditions B0–B2 are satisfied:

B0 on the history interval, $g(\xi(t))$ is non-zero and has the same sign as $g(\tilde{x}(t))$ for all $t \in [-\tau, 0] \setminus [\bigcup_{k=1}^{m}(\tilde{s}_k - \delta, \tilde{s}_k + \delta)]$,

and the headpoint trajectory $x(\cdot) = E(\cdot;\xi)(0) \subset \mathbb{R}^n$ satisfies

B1 $g(x(t))$ is non-zero and has the same sign as $g(\tilde{x}(t))$ for all $t \notin (\tilde{s}_k + lp - \delta, \tilde{s}_k + lp + \delta)$ $(l = 1, 2,\ k = 1, \ldots, m)$,

B2 $\|x(\tilde{s}_k + lp) - \tilde{x}(\tilde{s}_k)\| < \varepsilon$ for all $l = 1, 2$, $k = 1, \ldots, m$, and $\|x(2p) - \tilde{x}(0)\| < \varepsilon$.

A neighbourhood $\mathcal{N}$ satisfying the conditions B0–B2 above exists due to Condition 5, because E is continuous in $\tilde{x}$, and because $g(\tilde{x}(\cdot))$ has no zeroes in the compact set $[-p, 0] \setminus \bigcup_{k=1}^{m}(\tilde{s}_k - \delta, \tilde{s}_k + \delta)$.

Let $\xi \in \mathcal{N}$ be arbitrary, and $x(\cdot) = E(\cdot;\xi)(0)$ be its headpoint trajectory. Let $\tilde{s}_k$ $(k \in \{1, \ldots, \mu\})$ be one of the zeroes of $g(\tilde{x}(\cdot))$ in $[-p, 0]$ corresponding to the switching time $\tilde{t}_k$ and denote by Φ_j the flow that $\tilde{x}$ is following in $\tilde{s}_k$. Due to the conditions B0 and B1, $x(\cdot)$ also follows Φ_j in the intervals $(\tilde{s}_k + p - \delta, \tilde{s}_k + p + \delta)$ and $(\tilde{s}_k + 2p - \delta, \tilde{s}_k + 2p + \delta)$. Since $\|x(\tilde{s}_k + p) - \tilde{x}(\tilde{s}_k)\| < \varepsilon$ and $\|x(\tilde{s}_k + 2p) - \tilde{x}(\tilde{s}_k)\| < \varepsilon$, $g(x(\cdot))$ changes its sign and has exactly one zero in each of the intervals $(\tilde{s}_k + p - \delta, \tilde{s}_k + p + \delta)$ and $(\tilde{s}_k + 2p - \delta, \tilde{s}_k + 2p + \delta)$ due to condition B2.

Consequently, $g(x(\cdot))$ has exactly μ zeroes $s_1, \ldots, s_\mu \in [2p - 2\tau, 2p - \tau]$ (the same number as $g(\tilde{x}(\cdot))$), and $x(\cdot)$ follows Φ_1 in the time interval $(2p - \delta, 2p + \delta)$ (as does $\tilde{x}(\cdot)$). Thus, due to condition B2, $x(\cdot)$ also has a unique transversal intersection with the plane $\{\tilde{x}(0) + Lv : v \in \mathbb{R}^n\}$ at a time t_0 in a point $\tilde{x}(0) + Lv$. Then this v gives rise to the form (14) for $P^2 x$ where $t_k = (s_k + \tau) - t_0$ $(k = 1, \ldots, \mu)$. □

Appendix C. Proof of Theorem 9 in section 5

The proof of Theorem 9 requires several steps which we will follow through in the form of several lemmas. Let us denote by Φ_1 the flow corresponding to $\dot{x} = A(x + v)$ and by Φ_2 the flow corresponding to $\dot{x} = A(x - v)$ (following the notation of the section 3). We observe that Φ_1 and Φ_2 are symmetric to each other with respect to rotation by π in the origin, that is,

$$\Phi_2(t; z) = -\Phi_1(t; -z) \tag{C.1}$$

for all $z \in \mathbb{R}^n$. The flow Φ_1 can be expressed as an affine map

$$\Phi_1(t; z) = \exp(At)z + [\exp(At) - I]v \tag{C.2}$$

for $z \in \mathbb{R}^n$ and $t \in \mathbb{R}$. The equilibrium of the flow Φ_1 is at $-v$ and is of saddle type. There exist nonzero invariant projections P_+ and P_- corresponding to the stable (P_-) and unstable (P_+) eigenspaces of A such that $P_- + P_+ = I$. Let us assume (without loss of generality) that the basis of $\mathbb{R}^n$ is chosen such that $\|P_\pm\| = 1$ and, for certain constants $K_2 > K_1 > 0$, the dichotomy inequalities

$$\begin{array}{rcccl} \exp(K_2 t)\|P_+ z\| & \geq & \|P_+ \exp(At)z\| & \geq & \exp(K_1 t)\|P_+ z\| \\ \exp(-K_1 t)\|P_- z\| & \geq & \|P_- \exp(At)z\| & \geq & \exp(-K_2 t)\|P_- z\| \end{array} \tag{C.3}$$

hold for all $t \in \mathbb{R}$ and $z \in \mathbb{R}^n$ in the original Euclidean norm of $\mathbb{R}^n$.

Let m be an even number greater than $n + 1$. We now construct a g that gives rise to a slowly oscillating periodic orbit intersecting the switching manifold $\{g = 0\}$ transversally m times. More precisely, the periodic orbit switches m times between the two flows Φ_1 and Φ_2 and the time between successive switches is always greater than the delay τ of the switch.

Lemma 14
Let $\delta > 0$ be sufficiently small and denote by $B_\delta := \{z \in \mathbb{R}^n : \|P_- z - P_- v\| < \delta$ and $\|P_+ z + P_+ v\| < \delta\}$. Then there exist m-tuples $(\theta_1 \ldots, \theta_m) \in \mathbb{R}^m$ and $(x_1, \ldots, x_m) \in (\mathbb{R}^n)^m$ such that

(i) $\theta_j > \tau$ *for all* $j = 1, \ldots, m$,

(ii) $x_j \in B_\delta$ *for all* $j = 1, \ldots, m$,

(iii) $x_{j+1} = -\Phi_1(\theta_j; x_j)$ *for* $j = 1, \ldots, m-1$ *and* $x_1 = -\Phi_1(\theta_m; x_m)$,

(iv) the curves $\Phi_1([0, \theta_j]; x_j)$ *for* $j = 1, \ldots, m$ *are mutually disjoint, and,*

(v) using the notation $r_j = \theta_j + \ldots + \theta_m$ *($j = 1, \ldots, m$), the n vectors x_1, v,* $\exp(r_m A)v, \ldots,$ $\exp(r_{m-n+3} A)v$ *are linearly independent.*

Remark: We often use sets indexed by $j = m - n + 3, \ldots, m$ throughout this section (for example in point (v) above). For $n = 2$ these sets are meant to be empty.

Proof: Let $\theta_1, \ldots, \theta_m$ be larger than τ. A tuple $(x_1, \ldots, x_m) \in (\mathbb{R}^n)^m$ has property (iii) if and only if it satisfies the linear system of equations

$$\begin{aligned} x_{j+1} &= -[\exp(A\theta_j)x_j + (\exp(A\theta_j) - I)v] \quad \text{for } j = 1 \ldots, m-1, \\ x_1 &= -[\exp(A\theta_m)x_m + (\exp(A\theta_m) - I)v]. \end{aligned} \tag{C.4}$$

Using the invariant projections P_+ and P_- we can split (C.4) into an equivalent pair of systems of equations for $P_- x_j$ and $P_+ x_j$ ($j = 1, \ldots, m$):

$$\begin{aligned} P_- x_{j+1} &= P_- v - \exp(A\theta_j)(P_- x_j + P_- v) \quad \text{for } j = 1 \ldots, m-1, \\ P_- x_1 &= P_- v - \exp(A\theta_m)(P_- x_m + P_- v), \\ P_+ x_j &= -P_+ v - \exp(-A\theta_j)(P_+ x_{j+1} - P_+ v) \quad \text{for } j = 1 \ldots, m-1, \\ P_+ x_m &= -P_+ v - \exp(-A\theta_m)(P_+ x_1 - P_+ v) \end{aligned} \tag{C.5}$$

where the recursion for $P_+ x_j$ follows from (C.4) after premultiplication with $\exp(-\theta_j A)$. If the $\theta_1, \ldots, \theta_m$ are sufficiently large, the linear system (C.5) is a small perturbation of the regular system

$$\begin{aligned} P_- x_j &= P_- v \quad \text{for } j = 1 \ldots, m, \\ P_+ x_j &= -P_+ v \quad \text{for } j = 1 \ldots, m, \end{aligned} \tag{C.6}$$

due to the dichotomy inequalities (C.3). Consequently, we can find a $\theta_0 > \tau$ such that, for any tuple $(\theta_j)_{j=1}^m$ of numbers greater than θ_0, the perturbed system (C.5) (and, hence, (C.4)) is uniquely solvable and such that its solution has a distance less than δ from the solution of the unperturbed system (C.6). Thus, for any tuple $(\theta_j)_{j=1}^m$ of numbers greater than θ_0 we find a unique tuple $(x_j)_{j=1}^m$ that meets the properties (ii) and (iii) in the lemma. For a sufficiently small δ let the time T_δ be bigger than

$$\sup\{t \geq 0 : \Phi_1(t; B_\delta) \cap B_\delta \neq \emptyset\} + \sup\{t \geq 0 : \Phi_1(t; -B_\delta) \cap -B_\delta \neq \emptyset\}.$$

Both summands are finite since $-v$ (the equilibrium of Φ_1) is neither in B_δ nor in $-B_\delta$ due to the controllability of the pair (A, v). In fact, T_δ becomes smaller when δ gets smaller. If the tuple $(\theta_j)_{j=1}^m$ is chosen such that each two members of the tuple differ by more than T_δ then all curves $\Phi_1([0, \theta_1]; x_1), \ldots, \Phi_1([0, \theta_m]; x_m)$ are mutually disjoint. If, in addition, all θ_j ($j = 1, \ldots, m$) are greater than θ_0 then the assertions (ii)–(iv) of the lemma are satisfied simultaneously.

Let us finally adapt the tuple $(\theta_j)_{j=1}^m$ (and, thus, simultaneously $(x_j)_{j=1}^m$ defined by (C.4)) further to achieve property (v). Due to the controllability of the pair (A, v) we can find, for any $(m-1)$-tuple $(\theta_j)_{j=2}^m$, a $(m-1)$-tuple nearby such the set

$$\Sigma = \{v, \exp(r_m A)v, \ldots, \exp(r_{m-n+3} A)v\}$$

of $n-1$ vectors spans a $(n-1)$-dimensional space (where $r_j = \theta_j + \ldots + \theta_m$). The elements of Σ appear in assertion (v) in addition to x_1. We solve system (C.4) to obtain the representation

$$x_1 = [I - \exp(r_1 A)]^{-1} \left[\exp(r_1 A)v - 2\exp(r_2 A)v + - + \ldots - 2\exp(r_m A)v + v\right] \tag{C.7}$$

for the point x_1. The matrix $I - \exp(r_1 A)$ is regular because A has no eigenvalues on the imaginary axis. It remains to be shown that we can find an arbitrarily small adjustment of the m-tuple $(\theta_1, \ldots \theta_m)$ (or, equivalently, $(r_1, \ldots, r_m)$) that makes x_1 independent of the span of Σ.

We observe that r_2 can be varied without changing Σ. The vector x_1 has the form $x_1 = M[w - 2\exp(r_2 A)v]$ where $w \in \mathbb{R}^n$ and $M = [I - \exp(r_1 A)]^{-1}$ is a regular matrix. The controllability of the pair (A, v) implies the following: we can find a n-tuple of times $(t_1, \ldots, t_n)$ such that all t_j are close to r_2 and such that the set of vectors $\{w - 2\exp(t_1 A)v, \ldots, w - 2\exp(t_n A)v\}$ spans the whole $\mathbb{R}^n$. Consequently, $M[w - 2\exp(t_j A)v]$ must be independent of the span of Σ (which is $(n-1)$-dimensional) for one $t_j \approx r_2$. Thus, the small modification of the tuple $(\theta_1, \ldots, \theta_m)$ such that r_2 changes to t_j and $r_1, r_3, \ldots r_m$ (and, thus, Σ and M) remain unchanged guarantees that x_1 is independent of the span of Σ. Hence, with this small modification $(\theta_1, \ldots, \theta_m)$, along with the tuple $(x_1, \ldots, x_m)$ given by (C.4), also satisfies property (v). □

Corollary 15 *For tuples $(\theta_1, \ldots \theta_m)$ and $(x_1, \ldots, x_m)$ having the properties (iii) and (v) from Lemma 14 the sets $\{\exp(r_j A)x_j, v, \exp(r_m A)v, \ldots, \exp(r_{m-n+3} A)v\}$ are linearly independent (using the notation $r_j = \theta_j + \ldots + \theta_m$ for $j = m - n + 3, \ldots, m$).*

The statement of Corollary 15 follows recursively for $j = m, m-1, \ldots, m-n+3$ from system (C.4).

Due to the symmetry (C.1), the m-tuple $(x_1, \ldots, x_m)$ constructed in Lemma 14 defines a closed curve Ψ in $\mathbb{R}^n$ that follows trajectories of Φ_1 and Φ_2 in alternating fashion and switches at x_j (for odd j) from Φ_2 to Φ_1 and at $-x_j$ (for even j) from Φ_1 to Φ_2. We denote the smooth segments of the closed curve Ψ by Ψ_j for odd j and $-\Psi_j$ for even j:

$$\begin{aligned}
\Psi = \;& \Psi_1 \cup (-\Psi_2) \cup \ldots \Psi_{m-1} \cup (-\Psi_m) \\
= \;& \Phi_1([0, \theta_1]; x_1) \cup (-\Phi_1([0, \theta_2]; x_2)) \cup \ldots \\
& \cup \Phi_1[0, \theta_{m-1}]; x_{m-1}) \cup (-\Phi_1([0, \theta_m]; x_m)) \\
= \;& \Phi_1([0, \theta_1]; x_1) \cup \Phi_2([0, \theta_2]; -x_2) \cup \ldots \\
& \cup \Phi_1[0, \theta_{m-1}]; x_{m-1}) \cup \Phi_2([0, \theta_m]; -x_m).
\end{aligned} \tag{C.8}$$

The curve Ψ is continuous (by construction of $(x_1, \ldots, x_m)$; see Equation (C.4)) and piecewise smooth. It can only be non-differentiable at its joints x_1, $-x_2$, x_3, …, x_{m-1}, $-x_m$.

In the next step we show how to find, for sufficiently small δ, an appropriate switching function g such that Ψ is a slowly oscillating periodic orbit of the differential equation (21).

Lemma 16 *Let $\delta > 0$ be sufficiently small. Let the tuples $(\theta_1, \ldots, \theta_m)$ and $(x_1 \ldots, x_m)$ be as constructed in Lemma 14 and the closed curve $\Psi \subset \mathbb{R}^n$ be as defined in (C.8). Define the m points $\tilde{x}_j = \Phi_1(\theta_j - \tau; x_j)$ and let the vectors $\tilde{\beta}_j$ $(j = 1, \ldots, m)$ be such that*

$$\tilde{\beta}_j^T A[\tilde{x}_j + v] \neq 0. \tag{C.9}$$

Then there exists a smooth function g such that $g(-v) < 0$, $g(v) > 0$ and such that $\{g = 0\}$ is a manifold which partitions $\mathbb{R}^n$ into two simple domains and which intersects Ψ transversally exactly once in each of its smooth segments. Moreover,

- *for odd j, $\{g = 0\}$ intersects the segment Ψ_j in $\tilde{x}_j$ and its tangential hyperplane has the normal vector $\tilde{\beta}_j$, and*
- *for even j, $\{g = 0\}$ intersects the segment $-\Psi_j$ in $-\tilde{x}_j$ and its tangential hyperplane has the normal vector $-\tilde{\beta}_j$*

Property (i) in the construction of Lemma 14 guarantees that $\tilde{x}_j$ lies on Ψ_j for $j = 1, \ldots, m$). Condition (C.9) guarantees that the affine hyperplane attached to $\tilde{x}_j$ with normal vector $\tilde{\beta}_j$ in $\tilde{x}_j$ is indeed transversal to the segment Ψ_j in $\tilde{x}_j$.

PROOF: It is sufficient to construct two simple domains, G_1 for the flow Φ_1 and G_2 for the flow Φ_2, and a smooth boundary b separating them. Then, a smooth function g can always be chosen such that the interior of G_1 is $\{g < 0\}$ and the closure of G_2 is $\{g \geq 0\}$. For any sufficiently small $\varepsilon > 0$ we can choose a manifold b_0 such that (using the notation $B_\varepsilon(z)$ for the open ball of radius ε around $z \in \mathbb{R}^n$)

- b_0 has the form $\{z : \beta_0^T(z - \tilde{x}_0) = 0\}$ in the ball $B_\varepsilon(\tilde{x}_0)$ where $\tilde{x}_0 = \Phi_1(-\tau; P_+v - P_-v)$ and β_0 is chosen such that b_0 intersects all trajectories of Φ_1 transversally in $B_\varepsilon(\tilde{x}_0)$;
- b_0 has the form $\{z : -\beta_0^T(z - \tilde{x}_0) = 0\}$ in the ball $-B_\varepsilon(\tilde{x}_0)$, thus, b_0 intersects all trajectories of Φ_2 transversally in $-B_\varepsilon(\tilde{x}_0)$;
- b_0 has a positive distance from the ε-neighbourhoods of the affine subspaces $V_1 = \{z : P_-(z + v) = 0\}$ and $V_2 = \{z : P_-(z - v) = 0\}$
- the subspace V_1 (including the equilibrium $-v$ of Φ_1) lies on one side of b_0 and the subspace V_2 (including the equilibrium v of Φ_2) lies on the other side of b_0.

The balls $B_\varepsilon(\tilde{x}_0)$ and $-B_\varepsilon(\tilde{x}_0)$ do not intersect with the ε-neighbourhoods of V_1 and V_2 for sufficiently small ε. The transversality of the intersection of b_0 with $\Phi_1([-\infty, 0]; P_+v - P_-v)$ in $\tilde{x}_0$ implies that $\beta_0^T A[\tilde{x}_0 + v] \neq 0$.

Next we choose δ sufficiently small and the times of the tuple $(\theta_j)_{j=1}^m$ sufficiently large such that

- each of the segments Ψ_j intersects b_0 exactly once;
- all intersections of Ψ_j with b_0 occur in $B_\varepsilon(\tilde{x}_0)$ (let us denote these intersections by $\tilde{x}_j^0$, which are given by $\tilde{x}_j^0 = \Phi_1(\tilde{\theta}_j; x_j)$ for some $\tilde{\theta}_j \in (0, \theta_j)$);
- $\Phi_1(-\tau; -B_\delta) \subset B_\varepsilon(\tilde{x}_0)$, and, thus, $\tilde{x}_j = \Phi_1(\theta_j - \tau; x_j) = \Phi_1(-\tau; -x_{j+1}) \in B_\varepsilon(\tilde{x}_0)$ for $j = 1, \ldots, m$.

This choice of δ and $(\theta_j)_{j=1}^m$ is possible due the C^1-closeness of the segments $\Psi_1, \ldots, \Psi_m$ to the curve $\Phi_1((0, \infty]; -P_+v + P_-v) \cup \Phi_1([-\infty, 0]; P_+v - P_-v)$ outside of a small neighbourhood of $-v$ (the equilibrium of Φ_1) for large times $\theta_1, \ldots, \theta_m$. The construction of b_0 implies that, for even j, the segments $-\Psi_j$ intersect b_0 in $-B_\varepsilon(\tilde{x}_0)$. Furthermore, all intersections of b_0 with Ψ_j (j odd) and $-\Psi_j$ (j even) are transversal as they occur in $B_\varepsilon(\tilde{x}_0)$ and $-B_\varepsilon(\tilde{x}_0)$, respectively.

Finally, we modify b_0 in the interior of $B_\varepsilon(\tilde{x}_0)$ such that the modification b intersects Ψ_j in $\tilde{x}_j$ with normal vector $\tilde{\beta}_j$ (instead of intersecting Ψ_j in $\tilde{x}_j^0$ with normal vector β_0) for odd j. In exactly the same manner we also modify b_0 in the interior of $-B_\varepsilon(\tilde{x}_0)$ such that the modification b intersects $-\Psi_j$ in $-\tilde{x}_j$ with normal $-\tilde{\beta}_j$ (instead of intersecting $-\Psi_j$ in $-\tilde{x}_j^0$ with normal vector $-\beta_0$) for even j. An

additional restriction on the modification from b_0 to b is the requirement that b has to be transversal to all trajectories of Φ_1 in $B_\varepsilon(\tilde{x}_0)$ (and to all trajectories of Φ_2 in $-B_\varepsilon(\tilde{x}_0)$). We demonstrate that this modification can be achieved by following the flow Φ_1 from each point $z \in b_0 \cap B_\varepsilon(\tilde{x}_0)$ for an appropriate time $h(z)$ (and then apply the same procedure to $-B_\varepsilon(\tilde{x}_0)$).

Let $z \in U \subset \mathbb{R}^{n-1} \mapsto \tilde{x}_0 + Mz \in \mathbb{R}^n$ be a parametrization of $b_0 \cap B_\varepsilon(\tilde{x}_0) = \{\zeta \in B_\varepsilon(\tilde{x}_0) : \beta_0^T(\zeta - \tilde{x}_0) = 0\}$ where the matrix $M \in \mathbb{R}^{n\times(n-1)}$ has full rank $n-1$ and satisfies $\beta_0^T M = 0$. Then the intersection points $\tilde{x}_j^0$ of Ψ_j with b_0 have the form $\tilde{x}_j^0 = \tilde{x}_0 + Mz_j$ for a certain $z_j \in U$. We choose $h : C^\infty(\operatorname{clos} U; \mathbb{R})$ ($\operatorname{clos} U$ is the closure of U) such that

(i) $h(z_j) = \theta_j - \tau - \tilde{\theta}_j$ and, for $j = 1, 3, \ldots, m-1$,

$$h'(z_j) = \frac{-\tilde{\beta}_j^T \exp\left[A\left(\theta_j - \tau - \tilde{\theta}_j\right)\right] M}{\tilde{\beta}_j^T A[\tilde{x}_j + v]}, \tag{C.10}$$

(ii) $h(z) = 0$ and $h^{(k)}(z) = 0$ for all $z \in \partial U$ (the boundary of U) and $k \in \mathbb{N}$;

(iii) $\Phi_1(h(z); Mz + \tilde{x}_0) \in B_\varepsilon(\tilde{x}_0)$ for all $z \in \operatorname{clos} U$.

We choose the modified manifold b as $b = \{\Phi_1(h(z); Mz + \tilde{x}_0) : z \in U\} \cup (b_0 \setminus B_\varepsilon(\tilde{x}_0))$, which is, first, a smooth manifold due to the points (ii) and (iii) of the construction of h. Second, due to the smoothness of h, b is transversal to all trajectories of Φ_1 in $B_\varepsilon(\tilde{x}_0)$. Third, the manifold b intersects Ψ_j in $\tilde{x}_j$ and has the normal vector $\tilde{\beta}_j$ due to point (i) of the construction of h. Thus, after applying the analogous modification in $-B_\varepsilon(\tilde{x}_0)$ for even j, the manifold b is suitable as a switching manifold separating the domains of Φ_1 and Φ_2. □

For the g constructed in the proof of Lemma 16 the closed curve Ψ is a slowly oscillating periodic orbit that satisfies all genericity conditions postulated in section 4. The intersection points $\tilde{x}_j$ (for $j = 1, 3, \ldots, m-1$) and $-\tilde{x}_j$ (for $j = 2, 4, m$) are immediately followed by the corresponding switch at x_{j+1} and $-x_{j+1}$, respectively, without any intermediate crossing of the switching manifold $\{g = 0\}$. Thus, Poincaré maps along Ψ are, after symmetry reduction due to (C.1), concatenations of maps generated by following Φ_1 between the delayed switching manifolds and rotations by π. The choice of the cross-section for a Poincaré map does not affect the linearized stability of its fixed point corresponding to Ψ.

In the next step we choose the normal vectors $\tilde{\beta}_j$ (which are arbitrary in Lemma 16 apart from the transversality condition (C.9) in the construction of g) such that the linearization of a Poincaré map along Ψ becomes identically zero in its fixed point corresponding to Ψ. Equivalently, we can choose the normal vectors

$$\begin{aligned} \beta_{j+1}^T &= \tilde{\beta}_j^T \exp(-A\tau) \quad \text{for } j = 1, \ldots, m-1 \text{ and} \\ \beta_1^T &= \tilde{\beta}_m^T \exp(-A\tau) \end{aligned} \tag{C.11}$$

to the local delayed switching manifolds $\Phi_1(\tau; \{g = 0\}) \cap U(-x_j)$ in $-x_j$ for $j = 2, 4, \ldots, m$ and (after symmetry reduction) $-\Phi_1(\tau; -\{g = 0\}) \cap U(x_j)$ in x_j for $j = 1, 3, \ldots, m-1$. The transversality condition (C.9) on $\tilde{\beta}_j$ translates into the condition

$$\beta_j^T A[v - x_j] \neq 0 \tag{C.12}$$

for β_j and $j = 1, \ldots, m$. For any tuple $(\beta_j)_{j=1}^m$ satisfying (C.12), we find the corresponding tuple of normal vectors to the switching manifold at $(\tilde{x}_j)_{j=1}^m$, which is needed in the construction of g, by using the relation (C.11).

Let us choose a Poincaré section G_0 for Ψ through a point p on the segment $-\Psi_2$ (transversally to the curve $-\Psi_2$). Let the intersection time t_0 be such that t_0 is in the open interval $(0, \theta_2)$. The periodic orbit Ψ corresponds to a fixed point p of the return map. The return map along Ψ from G_0 to back G_0 has the simple form of a concatenation of maps between $(n-1)$-dimensional local hyper-surfaces of $\mathbb{R}^n$. The linearization of this concatenation in p contains the product of matrices

$$\Pi_2 \exp(\theta_1 A)(-I)\Pi_1 \exp(\theta_m A)(-I)\Pi_m \exp(\theta_{m-1} A) \cdot \ldots \cdot \Pi_{m-n+3} \tag{C.13}$$

where the maps Π_j are the discontinuity maps at the switching points x_j (after symmetry reduction). They are projections of the form

$$\Pi_j = I - \frac{A[v - x_j]\beta_j^T}{\beta_j^T A[v - x_j]},$$

which are well defined if the β_j satisfy the transversality condition (C.12). Thus, the kernel of Π_j is spanned by $A[v - x_j]$ and its image is $\{z \in \mathbb{R}^n : \beta_j^T z = 0\}$. Let us define the following recursion of matrices for j from m downward to $m - n + 3$:

$$P_1 := -\Pi_2 \exp(\theta_1 A)\Pi_1, \quad P_m = -P_1 \exp(\theta_m A)\Pi_m, \quad P_j := -P_{j+1} \exp(\theta_j A)\Pi_j$$

for $j < m$. The product (C.13) coincides with the final iterate P_{m-n+3} of this recursion. We now prove inductively that we can choose the vectors β_j ($j = 2, 1, m, m-1, \ldots, m-n+3$) defining Π_j such that

$$\begin{aligned} \ker P_1 &= A\mathcal{L}\left(x_1, v\right), \\ \ker P_m &= \exp(-r_m A) A\mathcal{L}\left(\exp(r_m A)x_m, v, \exp(r_m A)v\right) \\ &= A\mathcal{L}\left(x_m, v, \exp(-\theta_m A)v\right), \\ \ker P_j &= \exp(-r_j A) A\mathcal{L}\left(\exp(r_j A)x_j, v, \exp(r_m A)v, \ldots, \exp(r_j A)v\right) \end{aligned} \tag{C.14}$$

for $j = m-1, \ldots, m-n+3$ where the notation $\mathcal{L}(w_1, \ldots, w_k)$ refers to the subspace spanned by the vectors w_1, …, w_k. Lemma 14 and Corollary 15 imply that all sets on the right-hand-side of (C.14) are linearly independent. Thus, (C.14) implies that $\dim\ker P_{m-j} = j + 3$, and, hence, $P_{m-n+3} = 0$.

Initial step of induction ($j = 1$): Let β_2 be arbitrary but satisfying the transversality condition (C.12). The kernel of Π_2 is spanned by $A(v - x_2)$, which is non-zero. Thus, the kernel of $\Pi_2 \exp(\theta_1 A)$ is spanned by $\exp(-\theta_1 A)A(v - x_2) = A(v + x_1)$ (due to (C.4)). Because x_1 and v are linearly independent, so are $A(v+x_1)$ and $A(v-x_1)$ (since A is regular). Thus, we can choose β_1 such that $\beta_1^T A(v+x_1) = 0$ but $\beta_1^T A(v-x_1) \neq 0$ (thus, β_1 satisfies transversality condition (C.12)). The condition $\beta_1^T A(v + x_1) = 0$ implies that $\ker[\Pi_2 \exp(\theta_1 A)] \subset \mathrm{Im}\Pi_1$. Since $\ker\Pi_1 = \mathcal{L}(A(x_1 - v))$, this implies $\ker P_1 = \mathcal{L}(A[x_1 - v], A[x_1 + v]) = A\mathcal{L}(x_1, v)$. For $n = 2$ the product (C.13) is already identically zero.

Inductive step from $j+1$ to j (for $n \geq 3$)
Assumption. Assume that

$$\ker P_{j+1} = \exp(-r_{j+1} A) A\mathcal{L}\left(\exp(r_{j+1} A)x_{j+1}, v, \exp(r_m A)v, \ldots, \exp(r_{j+1} A)v\right). \tag{C.15}$$

Thus,

$$\begin{aligned} \ker[-P_{j+1} \exp(\theta_j A)] = \exp(-r_j A) A\mathcal{L}\left(\exp(r_{j+1} A)x_{j+1}, v, \exp(r_m A)v,\right. \\ \left. \ldots, \exp(r_{j+1} A)v\right). \end{aligned} \tag{C.16}$$

Step. The space spanned by the $m-j+3$ vectors

$$V = \mathcal{L}(\exp(r_j A)x_j, v, \exp(r_m A)v, \ldots, \exp(r_{j+1}A)v, \exp(r_j A)v) \tag{C.17}$$

has dimension $m-j+3$ as stated in Corollary 15. Thus, the same holds for $\exp(-r_j A)AV$, which can be split into the direct sum of the two components (separating the first and the last two vectors in the right-hand-side of (C.17) from the remaining $m-j$ vectors)

$$A\mathcal{L}(x_j, v, \exp(-\theta_j A)v) \oplus \exp(-r_j A)A\mathcal{L}(v, \exp(r_m A)v, \ldots, \exp(r_{j+2}A)v). \tag{C.18}$$

The first (three-dimensional) summand can be rewritten due to the identity $\exp(-A\theta_j)x_{j+1} = \exp(-A\theta_j)v - x_j - v$ following from (C.4):

$$\begin{aligned} A\mathcal{L}(x_j, v, \exp(-\theta_j A)v) = \\ &= A\mathcal{L}(x_j - v, \exp(-\theta_j A)x_{j+1}, \exp(-\theta_j A)v) \\ &= \mathcal{L}(A[x_j - v]) \oplus \exp(-r_j A)A\mathcal{L}\left(\exp(r_{j+1}A)x_{j+1}, \exp(r_{j+1}A)v\right). \end{aligned}$$

Recombining this with the second summand of the direct sum (C.18) of $\exp(-r_j A)AV$ gives the direct sum

$$\begin{aligned} \exp(-r_j A)AV \quad &= \mathcal{L}(A[x_j - v]) \oplus \exp(-r_j A)A\mathcal{L}\left(v, \exp(r_m A)v,\right. \\ &\quad \left. \ldots, \exp(r_{j+2}A)v, \exp(r_{j+1}A)v, \exp(r_{j+1}A)x_{j+1}\right). \end{aligned}$$

The second summand is by the assumption of the inductive step (C.16) the kernel of $P_{j+1}\exp(\theta_j A)$. The first summand is the kernel of Π_j. This implies that we can choose β_j such that $\beta_j^T A(x_j - v) \neq 0$ (thus, satisfying the transversality (C.12)) but $\beta_j^T z = 0$ for all $z \in [\ker P_{j+1}\exp(\theta_j A)]$, defining the map Π_j such that $\ker[P_{j+1}\exp(\theta_j A)] \subset \mathrm{Im}\Pi_j$. With this choice of β_j we have $\ker P_j = \ker[P_{j+1}\exp(\theta_j A)] \oplus \ker \Pi_j = \exp(-r_j A)AV$, which has dimension $m-j+3$ and assumes the form of (C.14) for j, thus, proving the inductive step. □

Consequently, if we choose the switching manifold as in the construction of Lemma 16 with $\tilde{\beta}_j$ given by (C.11) and the β_j as defined inductively above, the matrix product (C.13) has a kernel of dimension n and is, thus, zero. Hence, the linearization of the Poincaré map in G_0 for the periodic orbit Ψ has also vanishes. This implies that Ψ is quadratically stable, which proves Theorem 9.

Appendix D. Proof of Lemma 11

This section explains how the piecewise linearizations A_1 and A_2 in the statement of Lemma 11 depend on the right-hand-side and the concrete configuration of the periodic orbit $\tilde{x}$. Assume (without loss of generality) that $\tilde{x}$ follows Φ_1 for times smaller than $\tilde{s}_2$ and then switches to Φ_2 at $\tilde{s}_2$. Furthermore, we order the intersection times $-p < \tilde{s}_1 < \ldots < \tilde{s}_m < 0$ and denote the corresponding switching times by $\tilde{t}_1, \ldots, \tilde{t}_m$.

Case (a)
Let us denote $f_j^0 = f_j(\tilde{x}(\tilde{s}_2))$, $f_j^1 = f_j(\tilde{x}(\tilde{t}_2))$ where $j = 1, 2$ and $\tilde{t}_2 = \tilde{s}_2 + \tau$, and $g' = g'(\tilde{x}(\tilde{s}_2))$. Furthermore, let F_1 be the hyperplane intersecting $\tilde{x}$ in $\tilde{x}(\tilde{t}_2)$ orthogonal to the outgoing flow f_1^1. Let R be the return map along $\tilde{x}(\cdot)$ from F_1 to G_1^τ, which is a concatenation of smooth maps. We denote its derivative $\partial_x R|_{x=\tilde{x}(\tilde{t}_2)}$ by R'. Case (a) is defined in section 6.1 by $g' f_1^0 \cdot g' f_2^0 > 0$, which means that the periodic

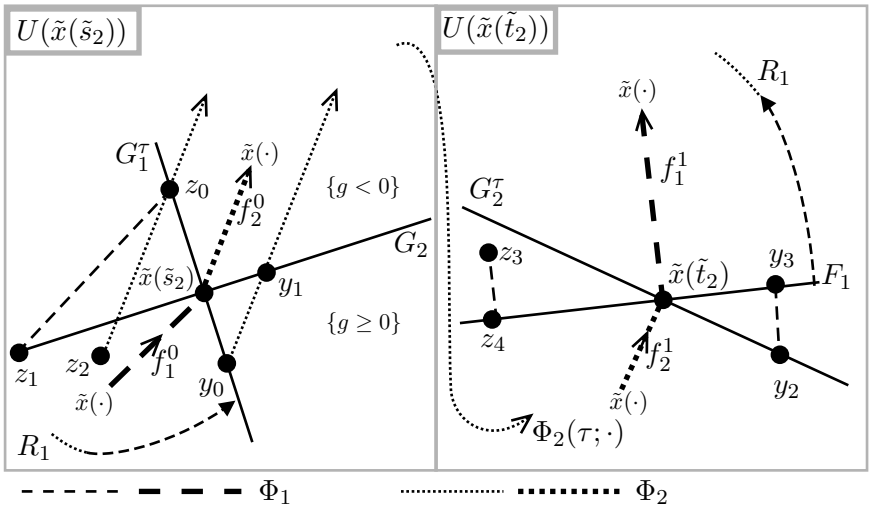

Figure D1. Sketch of the neighbourhoods $U(\tilde{x}(\tilde{s}_2))$ and $U(\tilde{x}(\tilde{t}_2))$ when $\tilde{x}(\cdot)$ undergoes a corner collision of type (a). Dashed trajectories follow flow Φ_1, dotted trajectories follow flow Φ_2. The return map P_0 is a concatenation of a non-smooth map from G_1^τ to F_1 and a smooth map R_1 from F_1 back to G_1^τ. The non-smooth map from G_1^τ to F_1 maps $\tilde{x}(\tilde{s}_2)$ to $\tilde{x}(\tilde{t}_2)$, $y_0 \in F_-$ to $y_3 \in F_1$, and $z_0 \in F_+$ to $z_4 \in F_1$.

orbit intersects the switching manifold $\{g = 0\}$ transversally. Figure D1 shows the configuration of the neighbourhood of $\tilde{x}(\tilde{s}_2)$ in the left panel. In this case there can be no other intersection or switching point on $\tilde{x}$ between $\tilde{s}_2$ and $\tilde{t}_2$. The maps A_1 (for $x + \tilde{x}(\tilde{s}_2) \in F_-$) and A_2 (for $x + \tilde{x}(\tilde{s}_2) \in F_+$) have the form

$$\begin{aligned} A_1 &= R' \left[I - \frac{f_1^1 {f_1^1}^T}{{f_1^1}^T f_1^1} \right] \partial_2 \Phi_2(\tau; \tilde{x}(\tilde{s}_2)) \left[I - \frac{f_2^0 g'}{g' f_2^0} \right] \\ A_2 &= R' \left[I - \frac{f_1^1 {f_1^1}^T}{{f_1^1}^T f_1^1} \right] \partial_2 \Phi_2(\tau; \tilde{x}(\tilde{s}_2)) \left[I - \frac{f_2^0 g'}{g' f_1^0} \right]. \end{aligned} \tag{D.1}$$

Notice that A_1 and A_2 differ only in the last factor. Let us first consider the case of a trajectory through a point $y_0 = \tilde{x}(\tilde{s}_2) + x \in F_-$ (see figure D1). It follows Φ_2 until it reaches G_2 in y_1. It continues to follow Φ_2 for time τ until it reaches G_2^τ, the time-τ image of G_2 in y_2 near $\tilde{x}(\tilde{s}_2)$ (see right panel of figure D1). The point y_3 is the projection of y_2 onto F_1 under Φ_1. The points y_1, y_2, and y_3 have the expansions

$$\begin{aligned} y_1 - \tilde{x}(\tilde{s}_2) &= \left[I - \frac{f_2^0 g'}{g' f_2^0} \right] x + \mathrm{O}(\|x\|^2), \\ y_2 - \tilde{x}(\tilde{t}_2) &= \partial_2 \Phi_2(\tau; \tilde{x}(\tilde{s}_2))(y_1 - \tilde{x}(\tilde{s}_2)) + \mathrm{O}(\|x\|^2), \\ y_3 - \tilde{x}(\tilde{t}_2) &= \left[I - \frac{f_1^1 {f_1^1}^T}{{f_1^1}^T f_1^1} \right] (y_2 - \tilde{x}(\tilde{s}_2)) + \mathrm{O}(\|x\|^2) \end{aligned}$$

giving the expression for A_1 in (D.1). A trajectory through a point $z_0 = \tilde{x}(\tilde{s}_2) + x \in F_+$ has crossed G_2 in z_1 at time δ, following Φ_1. Thus, the trajectory follows Φ_2 from z_0

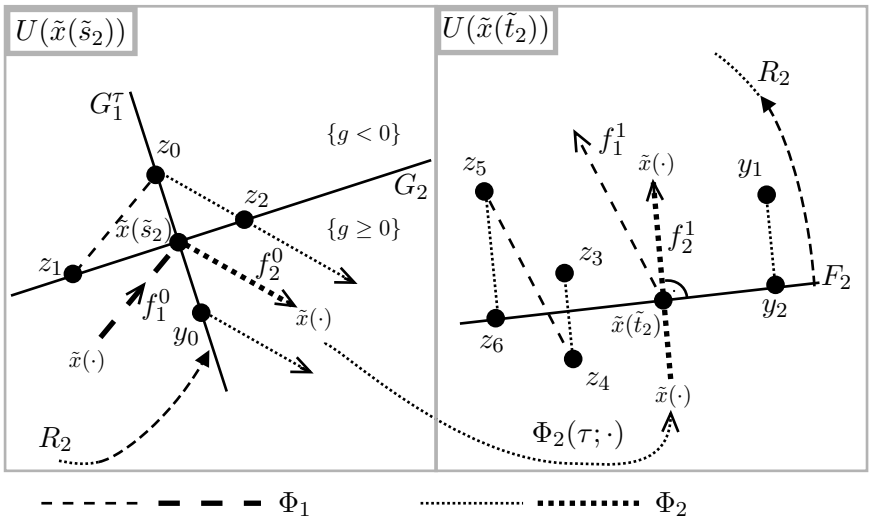

Figure D2. Sketch of the neighbourhoods $U(\tilde{x}(\tilde{s}_2))$ and $U(\tilde{x}(\tilde{t}_2))$ when $\tilde{x}(\cdot)$ undergoes a corner collision of type (b). The return map is a concatenation of a non-smooth map $G_1^\tau \mapsto F_2$ and the smooth map $R : F_2 \mapsto G_1^\tau$. The non-smooth map maps $\tilde{x}(\tilde{s}_2)$ to $\tilde{x}(\tilde{t}_2)$, $y_0 \in F_-$ to $y_2 \in F_2$ and $z_0 \in F_+$ to $z_6 \in F_2$.

up to $z_3 = \Phi_2(\tau; z_2)$ near $\tilde{x}(\tilde{s}_2)$ (see right panel of figure D1) where $z_2 = \Phi_2(\delta; z_0)$. The point z_4 is the projection of z_3 onto F_1 under Φ_1. The expansions of δ, z_2 to z_4 are

$$\begin{aligned}
\delta &= -g'x/(g'f_1^0) + \mathrm{O}(\|x\|^2),\\
z_2 - \tilde{x}(\tilde{s}_2) &= \left[I - \frac{f_2^0 g'}{g' f_1^0}\right] x + \mathrm{O}(\|x\|^2),\\
z_3 - \tilde{x}(\tilde{t}_2) &= \partial_2\Phi_2(\tau; \tilde{x}(\tilde{s}_2))(z_2 - \tilde{x}(\tilde{s}_2)) + \mathrm{O}(\|x\|^2),\\
z_4 - \tilde{x}(\tilde{t}_2) &= \left[I - \frac{f_1^1 {f_1^1}^T}{{f_1^1}^T f_1^1}\right] (z_3 - \tilde{x}(\tilde{s}_2)) + \mathrm{O}(\|x\|^2),
\end{aligned}$$

which implies the expression for A_2 in (D.1).

Case (b)
Let us denote $f_j^0 = f_j(\tilde{x}(\tilde{s}_2))$, $f_j^1 = f_j(\tilde{x}(\tilde{t}_2))$ where $j = 1, 2$ and $\tilde{t}_2 = \tilde{s}_2 + \tau$, and $g' = g'(\tilde{x}(\tilde{s}_2))$. Furthermore, let F_2 be the hyperplane intersecting $\tilde{x}$ in $\tilde{x}(\tilde{t}_2)$ orthogonal to the flow f_2^1. Let R be the return map along $\tilde{x}(\cdot)$ from F_2 to G_1^τ, which is a concatenation of smooth maps. We denote its derivative $\partial_x R|_{x=\tilde{x}(\tilde{t}_2)}$ by R'. Case (b) is defined in section 6.1 by $g'f_1^0 \cdot g'f_2^0 < 0$, which means that the periodic orbit lies entirely on one side of the switching manifold $\{g = 0\}$ near $\tilde{x}(\tilde{s}_2)$, touching it in $\tilde{x}(\tilde{s}_2)$. The left panel of figure D2 shows the configuration of the manifolds G_2, G_1^τ and the periodic orbit $\tilde{x}$ in the neighbourhood of $\tilde{x}(\tilde{s}_2)$. In addition, case (b) requires that the orbit $\tilde{x}$ does not intersect $\{g = 0\}$ between $\tilde{s}_2$ and $\tilde{t}_2$. The maps A_1 (for

$x + \tilde{x}(\tilde{s}_2) \in F_-$) and A_2 (for $x + \tilde{x}(\tilde{s}_2) \in F_+$) have the form

$$\begin{aligned} A_1 &= R' \left[I - \frac{f_2^1 {f_2^1}^T}{{f_2^1}^T f_2^1} \right] \partial_2 \Phi_2(\tau; \tilde{x}(\tilde{s}_2)), \\ A_2 &= R' \left[I - \frac{f_2^1 {f_2^1}^T}{{f_2^1}^T f_2^1} \right] \left\{ \partial_2 \Phi_2(\tau; \tilde{x}(\tilde{s}_2)) + \frac{f_1^1 g'}{g' f_1^0} - \frac{f_1^1 g'}{g' f_2^0} \right\}. \end{aligned} \tag{D.2}$$

Let us first consider a trajectory going through a point $y_0 = \tilde{x}(\tilde{s}_2) + x \in F_-$. It follows Φ_2 until it reaches F_2 in y_2. The point y_2 is the projection of $y_1 = \Phi_2(\tau; y_0)$ onto F_2 under Φ_2. The expansion for y_1 and y_2 is

$$\begin{aligned} y_1 - \tilde{x}(\tilde{t}_2) &= \partial_2 \Phi_2(\tau; \tilde{x}(\tilde{s}_2)) x + \mathrm{O}(\|x\|^2), \\ y_2 - \tilde{x}(\tilde{t}_2) &= \left[I - \frac{f_2^1 {f_2^1}^T}{{f_2^1}^T f_2^1} \right] (y_1 - \tilde{x}(\tilde{t}_2)) + \mathrm{O}(\|x\|^2), \end{aligned}$$

which, in concatenation with $R' : F_2 \mapsto G_1^\tau$, gives the expression for A_1 in (D.2). For a trajectory through a point $z_0 = \tilde{x}(\tilde{s}_2) + x \in F_+$ we have to compute the time that this trajectory spent in $\{g \geq 0\} \cap U(\tilde{x}(\tilde{s}_2))$, which is the traveling time $-\delta_1$ from z_1 to z_0 under Φ_1 plus the traveling time δ_2 from z_0 to z_2 under Φ_2 (see figure D2). The point z_3 is the $\Phi_2(\tau; \cdot)$-image of z_0. In the point $z_4 = \Phi_2(\delta_1; z_3)$ the trajectory switches to the flow Φ_1 for time $\delta_2 - \delta_1$, reaching z_5 where it switches back to Φ_2. The point z_6 is the projection of $z_5 = \Phi_1(\delta_2 - \delta_1; z_4)$ onto F_2 under Φ_2. The expansions of δ_1, δ_2, and z_3 to z_6 are

$$\begin{aligned} \delta_1 &= -g'x/(g' f_1^0) + \mathrm{O}(\|x\|^2), \quad (\delta_1 < 0), \\ \delta_2 &= -g'x/(g' f_2^0) + \mathrm{O}(\|x\|^2), \quad (\delta_2 > 0), \\ z_3 &= \tilde{x}(\tilde{t}_2) + \partial_2 \Phi_2(\tau; \tilde{x}(\tilde{s}_2)) x + \mathrm{O}(\|x\|^2), \\ z_4 &= z_3 + \delta_1 f_2^1 + \mathrm{O}(\|x\|^2), \\ z_5 &= z_4 + (\delta_2 - \delta_1) f_1^1 + \mathrm{O}(\|x\|^2), \\ z_6 &= \tilde{x}(\tilde{t}_2) + \left[I - \frac{f_2^1 {f_2^1}^T}{{f_2^1}^T f_2^1} \right] (z_5 - \tilde{x}(\tilde{t}_2)) + \mathrm{O}(\|x\|^2), \end{aligned}$$

which implies the expression for A_2 in (D.2) because the difference between z_3 and z_4 is in the kernel of the projection onto the hyperplane F_2.

Case (c)

In this case four locations in the physical space are involved in determining the discontinuity in the linearization of the Poincaré map $P_0 : G_1^\tau \mapsto G_1^\tau 0$: $U(\tilde{x}(\tilde{s}_2))$, $U(\tilde{x}(\tilde{s}_3))$, $U(\tilde{x}(\tilde{t}_2))$ and $U(\tilde{x}(\tilde{t}_3))$. A characteristic feature of this case is that the orbit $\tilde{x}$ crosses the switching manifold between $\tilde{s}_2$ and $\tilde{t}_2 = \tilde{s}_2 + \tau$ (in $\tilde{s}_3$; see figure 4(c)). Locally near $\tilde{x}(\tilde{s}_2)$, the orbit $\tilde{x}$ lies entirely on one side of $\{g = 0\}$, say, $\{g \geq 0\}$, switching from Φ_1 to Φ_2 in $\tilde{s}_2$. Figure D3 shows the four neighbourhoods.

Let us denote $f_j^0 = f_j(\tilde{x}(\tilde{s}_2))$, $f_j^1 = f_j(\tilde{x}(\tilde{s}_3))$, $f_j^2 = f_j(\tilde{x}(\tilde{t}_2))$, and $f_j^3 = f_j(\tilde{x}(\tilde{t}_3))$ where $j = 1, 2$ and $\tilde{t}_k = \tilde{s}_k + \tau$ $(k = 2, 3)$. Furthermore, let $g_0' = g'(\tilde{x}(\tilde{s}_2))$ and $g_1' = g'(\tilde{x}(\tilde{s}_3))$, and F_3 be the hyperplane intersecting $\tilde{x}$ in $\tilde{t}_3$ orthogonal to the outgoing flow Φ_1. The intersection and switching manifolds are called $G_1^\tau = \Phi_1(\tau; \{g = 0\}) \cap U(\tilde{x}(\tilde{s}_2))$, $G_2 = \{g = 0\} \cap U(\tilde{x}(\tilde{s}_2))$, $G_3 = \{g = 0\} \cap U(\tilde{x}(\tilde{s}_3))$ and $G_3^\tau = \Phi_2(\tau; \{g = 0\}) \cap U(\tilde{x}(\tilde{t}_3))$, respectively. We denote by Π_1 the projection along

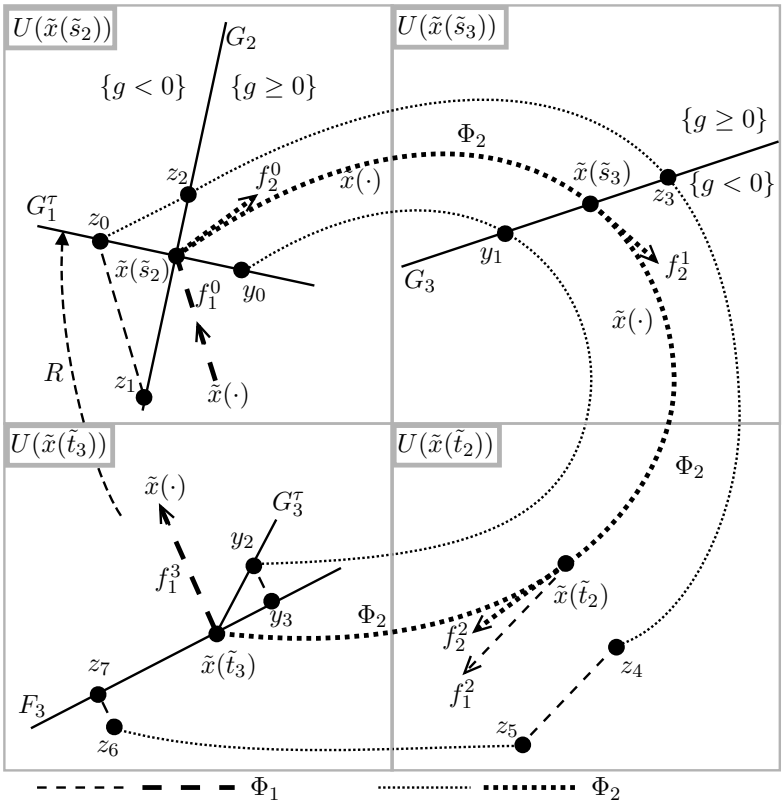

Figure D3. Sketch of the neighbourhoods $U(\tilde{x}(\tilde{s}_2))$, $U(\tilde{x}(\tilde{s}_3))$, $U(\tilde{x}(\tilde{t}_2))$ and $U(\tilde{x}(\tilde{t}_3))$ when $\tilde{x}(\cdot)$ undergoes a corner collision of type (c). The return map is a concatenation of the non-smooth map $G_1^\tau \mapsto F_3$, mapping y_0 to y_3 and z_0 to z_7, and the smooth map $R : F_3 \mapsto G_1^\tau$.

Φ_2 onto G_3, linearized in $\tilde{x}(\tilde{s}_3)$, and by Π_3 the projection along Φ_1 onto F_3, linearized in $\tilde{x}(\tilde{t}_3)$. The projections Π_1 and Π_3 read

$$\Pi_1 = I - \frac{f_2^1 g_1'}{g_1' f_2^1}, \quad \Pi_3 = I - \frac{f_1^3 {f_1^3}^T}{{f_1^3}^T f_1^3}.$$

Let R be the return map along $\tilde{x}(\cdot)$ from F_3 back to G_1^τ, which is a concatenation of smooth maps. We denote its derivative $\partial_x R|_{x=\tilde{x}(\tilde{t}_3)}$ by R'. We denote by $B_1 = \partial_2\Phi_2(\tilde{s}_3 - \tilde{s}_2; \tilde{x}(\tilde{s}_2))$, $B_2 = \partial_2\Phi_2(\tilde{t}_2 - \tilde{s}_3; \tilde{x}(\tilde{s}_3))$ and $B_3 = \partial_2\Phi_2(\tilde{t}_3 - \tilde{t}_2; \tilde{x}(\tilde{t}_2))$ the linearizations of the flow Φ_2 in $\tilde{x}$ between the different neighbourhoods. The vectors f_2^k satisfy the relations $f_2^1 = B_1 f_2^0$, $f_2^2 = B_2 B_1 f_2^0$, and $f_2^3 = B_3 B_2 B_1 f_2^0$. Using these notations, the piecewise linearizations in the statement of Lemma 11 are

$$A_1 = R'\Pi_3 B_3 B_2 \Pi_1 B_1,$$
$$A_2 = R'\Pi_3 B_3 \left\{ B_2 B_1 \left[I - \frac{f_2^0 g_1' B_1}{g_1' B_1 f_2^0} + \frac{f_2^0 g_0'}{g_0' f_2^0} - \frac{f_2^0 g_0'}{g_0' f_1^0} \right] + \left[\frac{f_1^2 g_0'}{g_0' f_1^0} - \frac{f_1^2 g_0'}{g_0' f_2^0} \right] \right\}. \tag{D.3}$$

Let us first consider a trajectory going through a point $y_0 = \tilde{x}(\tilde{s}_2) + x \in F_-$. It follows Φ_2 for time $\tau + \tilde{s}_3 - \tilde{s}_2$. The point y_1 is the intersection point of the trajectory

with G_3, y_2 is $\Phi_2(\tau; y_1)$, y_3 is the projection of y_2 onto F_3 under the flow Φ_1. This point y_3 is then mapped back to G_1^τ by R. The expansions of y_1, y_2 and y_3 read

$$\begin{aligned} y_1 - \tilde{x}(\tilde{s}_3) &= \Pi_1 B_1 x + \mathrm{O}(\|x\|^2), \\ y_2 - \tilde{x}(\tilde{t}_3) &= B_3 B_2 (y_1 - \tilde{x}(\tilde{s}_3)) + \mathrm{O}(\|x\|^2), \\ y_3 - \tilde{x}(\tilde{t}_3) &= \Pi_3 (y_2 - \tilde{x}(\tilde{t}_3)) + \mathrm{O}(\|x\|^2), \end{aligned}$$

which, in concatenation with $R' : F_3 \mapsto G_1^\tau$, gives the expression for A_1 in (D.3).

For a trajectory through a point $z_0 = \tilde{x}(\tilde{s}_2) + x \in F_+$ we have to compute the time that this trajectory spends in $\{g < 0\} \cap U(\tilde{x}(\tilde{s}_2))$, which is the traveling time $-\delta_1$ from z_1 to z_0 under Φ_1 plus the traveling time δ_2 from z_0 to z_2 under Φ_2 (the same as in case (b)). The point z_3 is the intersection point of the trajectory with G_3. The intersection time of the trajectory with G_3, starting from z_0, is $\tilde{s}_3 - \tilde{s}_2 + \delta_3$ for a small δ_3. In the point $z_4 = \Phi_2(\tau + \delta_1; z_0)$ the trajectory switches to the flow Φ_1, follows it for time $\delta_2 - \delta_1$ to z_5. From z_5 it continues to follow Φ_2 for time $\tilde{s}_3 - \tilde{s}_2 + \delta_3 - \delta_2$ to z_6. The point z_7 is the projection of z_6 onto F_3 under the flow Φ_1. This point z_7 is then mapped back to G_1^τ by R. The expansions of δ_1, δ_2, z_4 and z_5 are the same as in case (b), the expansion of δ_3, and z_4 to z_7 read

$$\begin{aligned} \delta_3 &= -g_1' B_1 x / (g_1' f_2^1) + \mathrm{O}(\|x\|^2), \\ z_4 &= \tilde{x}(\tilde{t}_2) + B_2 B_1 x + \delta_1 f_2^2 + \mathrm{O}(\|x\|^2), \\ &= \tilde{x}(\tilde{t}_2) + B_2 B_1 (x + \delta_1 f_2^0) + \mathrm{O}(\|x\|^2), \\ z_5 &= z_4 + (\delta_2 - \delta_1) f_1^2 + \mathrm{O}(\|x\|^2), \\ z_6 &= \tilde{x}(\tilde{t}_3) + B_3 (z_5 + (\delta_3 - \delta_2) f_2^2 - \tilde{x}(\tilde{t}_2)) + \mathrm{O}(\|x\|^2), \\ &= \tilde{x}(\tilde{t}_3) + B_3 B_2 B_1 \left[x + (\delta_3 - \delta_2 + \delta_1) f_2^0 \right] + B_3 (\delta_2 - \delta_1) f_1^2 + \mathrm{O}(\|x\|^2), \\ z_7 &= \tilde{x}(\tilde{t}_3) + \Pi_3 (z_6 - \tilde{x}(\tilde{t}_3)) + \mathrm{O}(\|x\|^2), \end{aligned}$$

which, in concatenation with $R' : F_3 \mapsto G_1^\tau$, gives the expression for A_2 in (D.3).

Appendix E. Proof of Lemma 13

Case (a)

The characteristic feature of case (a) is that the orbit $\tilde{x}$ does not cross the switching manifold between the grazing time s_* and $t_* = s_* + \tau$. Furthermore, let us assume that the configuration is such that the orbit $\tilde{x}$ does not switch from Φ_1 to Φ_2 between s_* and t_*, either; see figure E1 where we use the abbreviations $f^0 = \dot{\tilde{x}}(s_*) = f_1(\tilde{x}(s_*))$ and $f_j^1 = f_j(\tilde{x}(t_*))$. The hyperplane $F_1 = \{x : {f_1^1}^T [x - \tilde{x}(t_*)] = 0\}$ intersects $\tilde{x}$ orthogonally in $\tilde{x}(t_*)$. The linearized projection along Φ_1 onto F_1 defined by

$$\Pi = I - \frac{f_1^1 {f_1^1}^T}{{f_1^1}^T f_1^1}$$

is orthogonal. We express the return map to F_0 as a concatenation of a piecewise smooth map from F_0 to F_1 and a smooth map R along $\tilde{x}$ from F_1 back to F_0, which is a concatenation of smooth maps. Let us denote the derivative $\partial_x R(\tilde{x}(t_*))$ by R'. Using these notations the matrix A and the vector v in the statement of Lemma 13 have the form

$$\begin{aligned} A &= R' \Pi \partial_2 \Phi_1(\tau; \tilde{x}(s_*)) \\ v &= 2 R' \Pi f_2^1. \end{aligned} \tag{E.1}$$

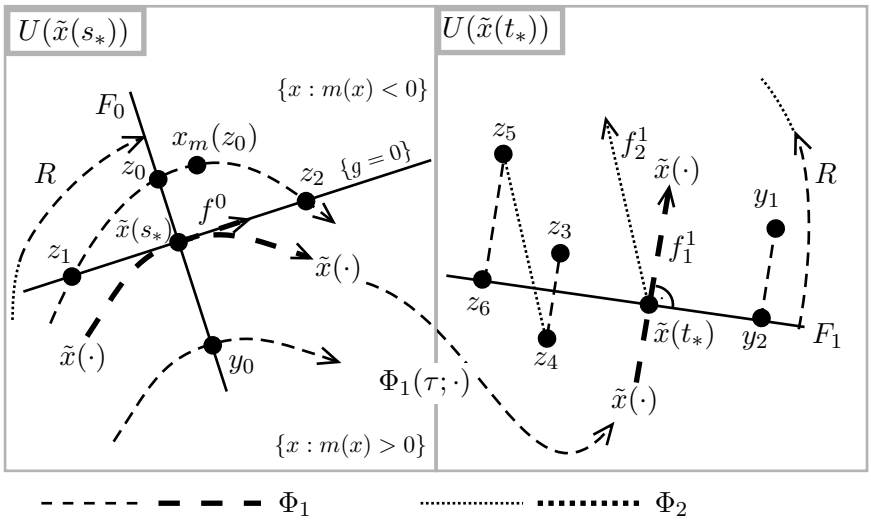

Figure E1. Sketch of the neighbourhoods $U(\tilde{x}(s_*))$ and $U(\tilde{x}(t_*))$ when $\tilde{x}(\cdot)$ undergoes a grazing bifurcation of type (a). The return map to F_0 is a concatenation of a non-smooth map $F_0 \mapsto F_1$ and a smooth map R. The non-smooth map maps $y_0 \in F_+$ to $y_2 \in F_1$ and $z_0 \in F_-$ to $z_6 \in F_1$.

Figure E1 illustrates how points of F_0 near $\tilde{x}(s_*)$ are mapped to F_1. A trajectory through a point $y_0 = \tilde{x}(s_*) + x \in F_+$ never crosses $\{g = 0\}$ in $U(\tilde{x}(s_*))$. Thus, it is mapped to $y_1 \in U(\tilde{x}(t_*))$ by $\Phi_1(\tau;\cdot)$. The point y_2 is the projection of y_1 onto F_1 under Φ_1. Thus, the expansion of y_2 with respect to y_0 is

$$y_1 - \tilde{x}(t_*) = \partial_2\Phi_1(\tau;\tilde{x}(s_*))x + \mathrm{O}(\|x\|^2),$$
$$y_2 - \tilde{x}(t_*) = \Pi(y_1 - \tilde{x}(t_*)) + \mathrm{O}(\|x\|^2),$$

which implies the expression for A in (E.1) in the case $\tilde{x}(\tilde{s}) + x \in F_+$.

The function $m : U(\tilde{x}(s_*)) \to \mathbb{R}$, used to define F_- and F_+ in Lemma 13, and defined by

$$m(x) = \min_{\delta\in[-\delta_0,\delta_0]} q^{-1}g(\Phi_1(\delta;x))$$

is uniquely defined and smooth for a sufficiently small $\delta_0 > 0$ due to Condition 12 (see page 18) stating the non-degeneracy of the grazing event. Moreover, the function

$$\delta_m : U(\tilde{x}(s_*)) \mapsto [-\delta_0,\delta_0], \text{ defined by } q^{-1}g(\Phi_1(\delta_m(x);x)) = m(x),$$

and the map

$$x_m(x) : U(\tilde{x}(s_*)) \mapsto U(\tilde{x}(s_*)), \text{ defined by } x_m(x) = \Phi_1(\delta_m(x);x),$$

are also well-defined and smooth in $U(\tilde{x}(s_*))$. The function δ_m describes the traveling time to the minimum in the definition of m. The map x_m describes the position in $\mathbb{R}^n$ where this minimum is attained. Thus, $\delta_m(\tilde{x}(s_*)) = 0$, which implies $\delta_m(\tilde{x}(s_*) + x) = \mathrm{O}(\|x\|)$, and $x_m(\tilde{x}(s_*)) = \tilde{x}(s_*)$.

A trajectory through $z_0 = \tilde{x}(s_*) + x \in F_-$ has two intersections z_1 and z_2 with $\{g = 0\}$. The traveling time from z_0 to $x_m(z_0)$ is $\delta_m(z_0)$. The traveling times $-\delta_1$ from

z_1 to $x_m(z_0)$ and δ_2 from $x_m(z_0)$ to z_2 are solutions of $h(\delta) := q^{-1}g(\Phi_1(\delta, x_m(z_0))) = 0$, which expands as

$$0 = h(\delta) = m(z_0) + \delta^2 + \mathrm{O}(\|x\|^2) + \mathrm{O}(\delta^3).$$

Thus, δ_1 and δ_2 have the expansions (keeping in mind that $m(z_0) = \mathrm{O}(\|x\|)$)

$$\delta_1 = -\sqrt{-m(z_0)} + \mathrm{O}(\|x\|),\ \delta_2 = \sqrt{-m(z_0)} + \mathrm{O}(\|x\|). \tag{E.2}$$

This implies that both, the traveling time from z_1 to z_0 and the traveling time from z_0 to z_2, are of the order $\sqrt{-m(z_0)} + \mathrm{O}(\|x\|)$ (because $\delta_m(z_0) = \mathrm{O}(\|x\|)$).

The trajectory through z_0 switches to the flow Φ_2 time $-\delta_1$ before it reaches the point

$$z_3 = \Phi_1(\tau; z_0) = \tilde{x}(t_*) + \mathrm{O}(\|x\|)$$

(see figure E1). This happens in point

$$z_4 = z_3 + \delta_1 f_1^1 + \mathrm{O}(\|x\|) = \tilde{x}(t_*) + \delta_1 f_1^1 + \mathrm{O}(\|x\|).$$

Subsequently the trajectory follows Φ_2 for time $\delta_2 - \delta_1$ up to

$$z_5 = z_4 + 2\sqrt{-m(z_0)} f_2^1 + \mathrm{O}(\|x\|) = \tilde{x}(t_*) + \delta_1 f_1^1 + 2\sqrt{-m(z_0)} f_2^1.$$

The point z_6 is the projection of z_5 onto F_1 under Π, which projects f_1^1 to 0. Thus, the expansion of z_6 is

$$\begin{aligned} z_6 &= \tilde{x}(t_*) + \Pi(z_5 - \tilde{x}(t_*)) + \mathrm{O}(\|x\|^2) \\ &= \tilde{x}(t_*) + \Pi[2f_2^1]\sqrt{-m(z_0)} + \mathrm{O}(\|x\|), \end{aligned}$$

which implies the expression for v in (E.1). □

If the orbit $\tilde{x}$ switches from Φ_1 to Φ_2 between s_* and t_* (at some time $\tilde{t}_1 \in (s_*, t_*)$ a modification of (E.1) applies. Since $\tilde{x}$ follows Φ_2 in t_* instead of Φ_1 the role of f_1^1 and f_2^1 is interchanged in the definition of Π and v. Furthermore, the time τ-map from $U(\tilde{x}(s_*))$ to $U(\tilde{x}(t_*))$ is no longer $\Phi_1(\tau, \cdot)$ but $R_0(x) = \Phi_2(\tau - t(x); \Phi_1(t(x); x))$ where $t(x)$ is the traveling time from x to the delayed switching manifold $G_1^\tau = \Phi_1(\tau; \{g = 0\}) \cap U(\tilde{x}(\tilde{t}_1))$. This traveling time depends smoothly on x, which implies that R_0 is smooth as well. With these modifications the arguments given above lead to

$$A = R' \left[I - \frac{f_2^1 {f_2^1}^T}{{f_2^1}^T f_2^1} \right] \partial_x R_0(\tilde{x}(s_*)), \quad v = 2R' \left[I - \frac{f_2^1 {f_2^1}^T}{{f_2^1}^T f_2^1} \right] f_1^1. \tag{E.3}$$

Case (b)

The characteristic feature of this case is that the orbit $\tilde{x}$ intersects the switching manifold $\{g = 0\}$ between s_* and t_* at some time $\tilde{s}_2$. Four locations in the physical space are involved in determining the discontinuity in the linearization of the Poincaré map P_0 from F_0 back to F_0: $U(\tilde{x}(s_*))$, $U(\tilde{x}(\tilde{s}_2))$, $U(\tilde{x}(t_*))$ and $U(\tilde{x}(\tilde{t}_2))$. Let us first assume that the orbit $\tilde{x}$ does not switch from flow Φ_1 to Φ_2 between s_* and $\tilde{s}_2$.

Figure E2 shows this configuration. It uses the abbreviations $f^0 = \dot{\tilde{x}}(s_*) = f_1(\tilde{x}(s_*))$, $f_j^1 = f_j(\tilde{x}(\tilde{s}_2))$, $f_j^2 = f_j(\tilde{x}(t_*))$ and $f_j^3 = f_j(\tilde{x}(\tilde{t}_2))$ for $j = 1, 2$. The hyperplane $F_3 = \{x : {f_2^3}^T[x - \tilde{x}(\tilde{t}_2)] = 0\}$ intersects $\tilde{x}$ orthogonal to the outgoing flow Φ_2 in $\tilde{x}(\tilde{t}_2)$. We denote by Π_1 the projection along Φ_1 onto $G_2 = \{g = 0\} \cap U(\tilde{x}(\tilde{s}_2))$, linearized in $\tilde{x}(\tilde{s}_2)$, and by Π_3 the projection along Φ_2 onto F_3, linearized in $\tilde{x}(\tilde{t}_2)$. The projections Π_1 and Π_3 read

$$\Pi_1 = I - \frac{f_1^1 g'(\tilde{x}(\tilde{s}_2))}{g'(\tilde{x}(\tilde{s}_2)) f_1^1}, \quad \Pi_3 = I - \frac{f_2^3 {f_2^3}^T}{{f_2^3}^T f_2^3}.$$

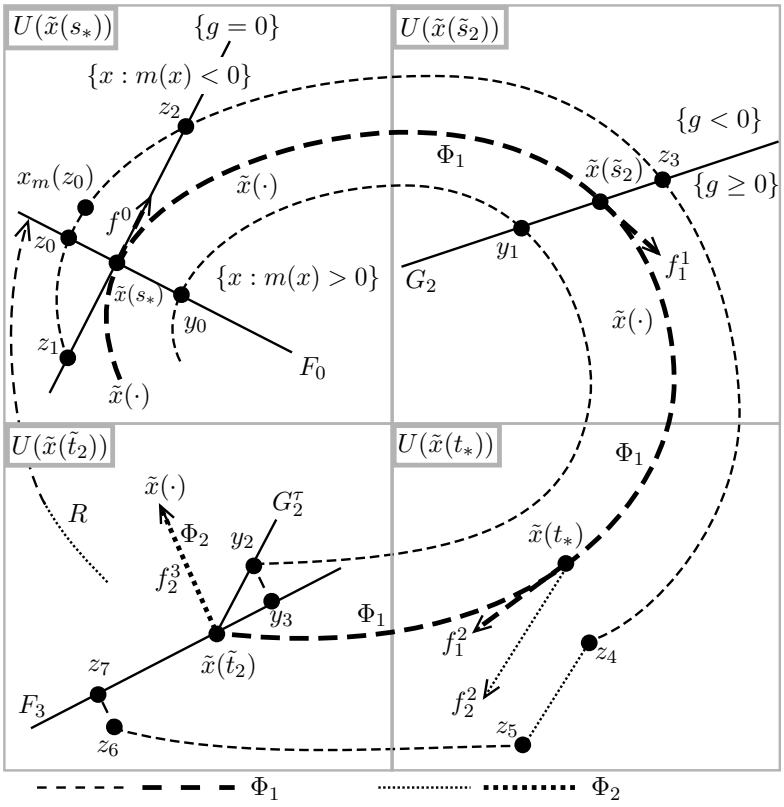

Figure E2. Sketch of the neighbourhoods $U(\tilde{x}(s_*))$, $U(\tilde{x}(\tilde{s}_2))$, $U(\tilde{x}(t_*))$ and $U(\tilde{x}(\tilde{s}_t))$ when $\tilde{x}(\cdot)$ undergoes a grazing bifurcation of type (b). The return map to F_0 is a concatenation of a non-smooth map $F_0 \mapsto F_3$ and a smooth map R. The non-smooth map maps $y_0 \in F_+$ to $y_3 \in F_3$ and $z_0 \in F_-$ to $z_7 \in F_3$.

We express the return map to F_0 as a concatenation of a piecewise smooth map from F_0 to F_3 and a smooth map R from F_3 back to F_0. The return map R along $\tilde{x}(\cdot)$ from F_3 back to F_0 is a concatenation of smooth maps. Let us denote its derivative $\partial_x R(\tilde{x}(\tilde{t}_2))$ by R'. We also make use of the function m defined in section 6.2 and discussed in more detail in the treatment of case (a).

Using these notations the matrix A and the vector v in the statement of Lemma 13 have the form

$$\begin{aligned} A &= R'\Pi_3\partial_2\Phi_1(\tau;\tilde{x}(s_2))\Pi_1\partial_2\Phi_1(\tilde{s}_2 - s_*;\tilde{x}(s_*)) \\ v &= 2R'\Pi_3\partial_2\Phi_1(\tilde{s}_2 - s_*;\tilde{x}(t_*))[f_2^2 - f_1^2]. \end{aligned} \tag{E.4}$$

A trajectory through a point $y_0 = \tilde{x}(s_*) + x \in F_+$ does not cross $\{g = 0\}$ in $U(\tilde{x}(s_*))$ (see figure E2). It is mapped to $y_1 \in G_2$ by Φ_1. The trajectory continues to follow Φ_1 for time τ from y_1 to y_2. The point y_3 is the projection of y_2 onto F_3 under Φ_2.

Thus, the expansion of y_1, y_2, y_3 with respect to y_0 is

$$\begin{aligned} y_1 - \tilde{x}(\tilde{s}_2) &= \Pi_1 \partial_2 \Phi_1(\tilde{s}_2 - s_*; \tilde{x}(s_*))x + \mathrm{O}(\|x\|^2), \\ y_2 - \tilde{x}(\tilde{t}_2) &= \partial_2 \Phi_1(\tau; \tilde{x}(\tilde{s}_2))(y_1 - \tilde{x}(\tilde{s}_2)), \\ y_3 - \tilde{x}(\tilde{t}_2) &= \Pi_3(y_2 - \tilde{x}(\tilde{t}_2)) + \mathrm{O}(\|x\|^2), \end{aligned}$$

which implies the expression for A in (E.4).

A trajectory through a point $z_0 = \tilde{x}(s_*) + x \in F_-$ has two intersection points with $\{g = 0\}$, z_1 and z_2 (see figure E2). The traveling times $-\delta_1$ from z_1 to z_0 and δ_2 from z_0 to z_2 have been computed to leading order already in (E.2) in the treatment of the grazing case (a). The intersection of the trajectory with G_2 is named z_3. The difference δ_3 between the traveling time from z_0 to z_3 and $\tilde{s}_2 - s_*$ is of order $\mathrm{O}(\|x\|)$. At $z_4 = \Phi_1(\tau + \delta_1; z_0)$ the trajectory switches to Φ_2 for time $\delta_2 - \delta_1$, reaching z_5. From z_5 it continues to follow Φ_1 for time $\tilde{t}_2 - t_* + \delta_3 - \delta_2 = \tilde{s}_2 - s_* - \delta_2 + \mathrm{O}(\|x\|)$ reaching z_6. The point $z_7 \in F_3$ is the projection of z_6 onto F_3 following the outgoing flow Φ_2, and is then mapped back to F_0 by R. The expansion of z_7 in z_0 is to leading order

$$\begin{aligned} &\delta_3 = \mathrm{O}(\|x\|), \\ &z_4 = \tilde{x}(t_*) + \delta_1 f_1^2 + \mathrm{O}(\|x\|), \\ &z_5 = z_4 + (\delta_2 - \delta_1) f_2^2 + \mathrm{O}(\|x\|)), \\ &z_6 = \tilde{x}(\tilde{t}_2) + \partial_2 \Phi_1(\tilde{s}_2 - s_*; \tilde{x}(t_*)) \left[z_5 - \delta_2 f_1^2 - \tilde{x}(t_*) + \mathrm{O}(\|x\|) \right] + \mathrm{O}(\|x\|), \\ &\quad = \tilde{x}(\tilde{t}_2) + \partial_2 \Phi_1(\tilde{s}_2 - s_*; \tilde{x}(t_*))(\delta_2 - \delta_1) \left[f_2^2 - f_1^2 \right] + \mathrm{O}(\|x\|), \\ &\quad = \tilde{x}(\tilde{t}_2) + 2\partial_2 \Phi_1(\tilde{s}_2 - s_*; \tilde{x}(t_*)) \left[f_2^2 - f_1^2 \right] \sqrt{-m(z_0)} + \mathrm{O}(\|x\|), \\ &z_7 = \tilde{x}(\tilde{t}_2) + \Pi_3[z_6 - \tilde{x}(\tilde{t}_2)] + \mathrm{O}(\|x\|), \end{aligned}$$

which implies the expression for v in (E.4).

If the orbit $\tilde{x}$ switches from Φ_1 to Φ_2 between s_* and $\tilde{s}_2$ (at some time $\tilde{t}_1 \in (s_*, \tilde{s}_2)$) a modification of (E.4) applies. Since $\tilde{x}$ follows Φ_2 in $\tilde{s}_2$ and t_* instead of Φ_1, and switches from Φ_2 to Φ_1 in $\tilde{t}_2$, the role of f_1^1 and f_2^1 is interchanged in the definition of Π_1, Π_3 and v. Furthermore, the time-$(s_* - \tilde{s}_2)$ map from $U(\tilde{x}(s_*))$ to $U(\tilde{x}(\tilde{s}_2))$ is no longer $\Phi_1(\tilde{s}_2 - s_*, \cdot)$ but $R_1(x) = \Phi_2(\tilde{s}_2 - s_* - t(x); \Phi_1(t(x); x))$ where $t(x)$ is the traveling time from x to the delayed switching manifold $G_1^\tau = \Phi_1(\tau; \{g = 0\}) \cap U(\tilde{x}(\tilde{t}_1))$. This traveling time depends smoothly on x, which implies that R_1 is smooth as well. With these modifications the derivation given above leads to

$$\begin{aligned} A &= R' \left[I - \frac{f_1^3 f_1^{3T}}{f_1^{3T} f_1^3} \right] \partial_2 \Phi_2(\tau; \tilde{x}(s_2)) \left[I - \frac{f_2^1 g'(\tilde{x}(\tilde{s}_2))}{g'(\tilde{x}(\tilde{s}_2)) f_2^1} \right] \partial_x R_1(\tilde{x}(s_*)), \\ v &= 2R' \left[I - \frac{f_1^3 f_1^{3T}}{f_1^{3T} f_1^3} \right] \partial_2 \Phi_2(\tilde{s}_2 - s_*; \tilde{x}(t_*))[f_1^2 - f_2^2]. \end{aligned} \tag{E.5}$$

This completes the proof of Lemma 13. □